Recognized as an
American National Standard (ANSI)

IEEE Std C62.47-1992

IEEE Guide on Electrostatic Discharge (ESD): Characterization of the ESD Environment

Circuits and Devices

Communications Technology

Computer

Electromagnetics and Radiation

IEEE Power Engineering Society

Sponsored by the
Surge-Protective Devices Committee

Industrial Applications

Signals and Applications

Standards Coordinating Committees

Published by the Institute of Electrical and Electronics Engineers, Inc., 345 East 47th Street, New York, NY 10017, USA.

March 16, 1993 SH15271

IEEE Std C62.47-1992

Recognized as an
American National Standard (ANSI)

IEEE
Std C62.47-1992

IEEE Guide on Electrostatic Discharge (ESD): Characterization of the ESD Environment

Sponsor

Surge-Protective Devices Committee
of the
IEEE Power Engineering Society

Approved March 19, 1992

IEEE Standards Board

Approved December 23, 1992

American National Standards Institute

Abstract: This guide describes the electromagnetic threat posed to electronic equipment and subassemblies by actual Electrostatic Discharge (ESD) events from humans and mobile furnishings. This guide organizes existing data on the subject of ESD in order to characterize the ESD surge environment. This guide is not an ESD test standard. It is intended to be a resource for equipment designers, and for preparers and users of ESD test standards. The manufacturing, handling, packaging, and transportation of individual electronic components, including integrated circuits, are not discussed, and this guide does not deal with mobile items such as automobiles, aircraft, or other masses of comparable size.

Keywords: electromagnetic, electrostatic discharge, ESD, surges

The Institute of Electrical and Electronics Engineers, Inc.
345 East 47th Street, New York, NY 10017-2394, USA

ISBN 1-55937-224-9

IEEE Standards documents are developed within the Technical Committees of the IEEE Societies and the Standards Coordinating Committees of the IEEE Standards Board. Members of the committees serve voluntarily and without compensation. They are not necessarily members of the Institute. The standards developed within IEEE represent a consensus of the broad expertise on the subject within the Institute as well as those activities outside of IEEE that have expressed an interest in participating in the development of the standard.

Use of an IEEE Standard is wholly voluntary. The existence of an IEEE Standard does not imply that there are no other ways to produce, test, measure, purchase, market, or provide other goods and services related to the scope of the IEEE Standard. Furthermore, the viewpoint expressed at the time a standard is approved and issued is subject to change brought about through developments in the state of the art and comments received from users of the standard. Every IEEE Standard is subjected to review at least every five years for revision or reaffirmation. When a document is more than five years old and has not been reaffirmed, it is reasonable to conclude that its contents, although still of some value, do not wholly reflect the present state of the art. Users are cautioned to check to determine that they have the latest edition of any IEEE Standard.

Comments for revision of IEEE Standards are welcome from any interested party, regardless of membership affiliation with IEEE. Suggestions for changes in documents should be in the form of a proposed change of text, together with appropriate supporting comments.

Interpretations: Occasionally questions may arise regarding the meaning of portions of standards as they relate to specific applications. When the need for interpretations is brought to the attention of IEEE, the Institute will initiate action to prepare appropriate responses. Since IEEE Standards represent a consensus of all concerned interests, it is important to ensure that any interpretation has also received the concurrence of a balance of interests. For this reason IEEE and the members of its technical committees are not able to provide an instant response to interpretation requests except in those cases where the matter has previously received formal consideration.

Comments on standards and requests for interpretations should be addressed to:

Secretary, IEEE Standards Board
445 Hoes Lane
P.O. Box 1331
Piscataway, NJ 08855-1331
USA

Foreword

(This foreword is not a part of IEEE Std C62.47-1992, IEEE Guide for Electrostatic Discharge (ESD): Characterization of the ESD Environment.)

An electrostatic discharge (ESD) event can cause equipment malfunction as well as physical damage. Equipment malfunction may include corruption of data and equipment lock-ups. Physical damage may include equipment damage and even loss of life.

In order to achieve meaningful ESD immunity, the design of an entire system must be considered, both for direct discharge and for fields. Various design tools are available to assist in increasing the ESD immunity of electronic equipment. The utility of these tools is limited, however, if the character of the ESD threat is not understood.

There are standards for simulating the ESD environment at the equipment level. They have been published by several organizations, including IEC and ECMA; others are in preparation, including one by ASC C63. However, much has been learned about ESD since early versions of some of these standards were published. In addition, all of these standards are exclusively test standards; repeatability has been a major goal, sometimes at the expense of realism. Therefore, these standards are not necessarily fully accurate sources of information regarding the ESD threat itself; presentation of such information is typically not their purpose.

To date, no other organization has written a guide that describes the characteristics of the real-world ESD event itself. This guide has been written to fill that void. *This guide is not an ESD test standard.* Rather, it is intended to be a resource for equipment designers, and for preparers and users of ESD test standards. This guide will allow all those who are responsible for ESD immunity to judge the relative realism of proposed ESD tests by comparing them to the real-world ESD events described.

The reader of this guide is encouraged to use an appropriate test standard to define actual ESD immunity tests for equipment.

At the time this guide was completed, the working group on ESD had the following membership:

Warren Boxleitner, *Chair*

Francis Drake	Ray D. Jones	Louis Shulman
Peter A. Goodwin	Mark T. Ma	Dennis Symanski
Phil Jedlicka	Edward H. Marrow	Arthur W. Woltman
	Bill Rhoades	

Other individuals who have contributed significant review and comments are:

G. J. Bagnall	J. E. Brunssen	Kevin Smith
	Peter Richman*	

*Initiated working group and served as chair until 1989.

At the time that it balloted and approved this standard for submission to the IEEE Standards Board, the Surge-Protective Devices Committee had the following membership:

G. J. Bagnall	G. S. Haralampu	M. Parente
W. Boxleitner	J. L. Koepfinger	P. Richman
D. C. Dawson	W. A. Maguire	L. D. Sweeney
G. L. Gaibrois	E. H. Marrow, Jr.	D. P. Symanski
P. A. Goodwin	F. D. Martzloff	E. R. Taylor, Jr.
	R. Odenberg	

When the IEEE Standards Board approved this standard on March 19, 1992, it had the following membership:

Marco W. Migliaro, Chair **Donald C. Loughry,** *Vice Chair*
Andrew G. Salem, *Secretary*

Dennis Bodson
Paul L. Borrill
Clyde Camp
Donald C. Fleckenstein
Jay Forster*
David F. Franklin
Ramiro Garcia
Thomas L. Hannan
Donald N. Heirman
Ben C. Johnson
Walter J. Karplus
Ivor N. Knight
Joseph Koepfinger*
Irving Kolodny
D. N. "Jim" Logothetis
Lawrence V. McCall
T. Don Michael*
John L. Rankine
Wallace S. Read
Ronald H. Reimer
Gary S. Robinson
Martin V. Schneider
Terrance R. Whittemore
Donald W. Zipse

*Member Emeritus

Also included are the following nonvoting IEEE Standards Board liaisons:

Satish K. Aggarwal
James Beall
Richard B. Engelman
Stanley Warshaw

Mary Lynne Nielsen
IEEE Standards Project Editor

Grateful acknowledgment is made to the following for having granted permission to reprint material in this document as listed below:

Information in Table 3 was taken from Table 1 of "An ESD Circuit Model with Initial Spikes to Duplicate Discharges from Hands with Metal Objects," published in *EMC Technology*, vol. 4, no. 2, pp. 53–59, Apr.–Jul. 1985. Owned by *EMC Technology* magazine. Permission to reproduce is required from EMCT.

Figs 21, 22, 24, and 25 were taken from Weil, G., "Making Accurate and Repeatable Measurements of the ESD Current Waveform in the Regime of 1 GHz and Above," in *Proceedings of the 8th EMC Symposium*, pp. 355–360, 1989.

Figs B10, B11, and B12 were taken from Daout, B., Ryser, H., Germond A., and Zweiacker, P., "The Correlation of Rising Slope and Speed of Approach in ESD Tests," in *Proceedings of the 7th EMC Symposium on EMC*, pp. 461–466, 1987.

Contents

SECTION PAGE

APPENDIXES

FIGURES

SECTION PAGE

TABLES

APPENDIX FIGURES

APPENDIX TABLES

IEEE Guide on Electrostatic Discharge (ESD): Characterization of the ESD Environment

1. Scope and Purpose

The purpose of this guide is to describe the electromagnetic threat posed to electronic equipment and subassemblies by actual Electrostatic Discharge (ESD) events from humans and mobile furnishings. This guide organizes existing data on the subject of ESD in order to characterize the ESD surge environment. This guide is not an ESD test standard. An appropriate ESD test standard should be selected for equipment testing ([1], [3], [B1]).[1]

The manufacturing, handling, packaging, and transportation of individual electronic components, including integrated circuits, are not discussed, and this guide does not deal with mobile items such as automobiles, aircraft, or other masses of comparable size.

ESD results in a sudden transfer of charge between bodies of differing electrostatic potentials. In this guide, the term ESD includes charge transfer whether or not an arc occurs or is perceived.

ESD phenomena generate electromagnetic fields over a broad range of frequencies, from direct current (dc) to low gigahertz. The term *ESD event* includes not only the discharge current, but also the electromagnetic fields and corona effects before and during a discharge.

In this guide the intruder is often a human, but it may be any object that is moved, such as a chair, an equipment cart, a vacuum cleaner, or the equipment victim itself, whether or not it is in conductive contact with a human. The equipment victim is usually a fabricated electronic equipment or subassembly and is generally, although not necessarily, at local electrostatic ground potential.

The equipment victim may be the receptor to which the discharge takes place from the intruder; less frequently, the equipment victim may be the intruder. Alternatively, the equipment victim may be affected by the electromagnetic fields generated by a discharge between an intruder and a receptor. Receptors and intruders that may not themselves be equipment victims include furniture such as metal chairs, carts, tables and file cabinets, as well as other electronic equipment.

This guide discusses and cites references that describe the ways in which a body builds up charge and the characteristics of discharge currents and fields. Descriptions and references are also given for electrical equivalent circuits to be used in understanding and simulating the discharge current between intruder and receptor masses.

Publications that are specifically referenced in the text of the guide are listed in the Section 3, while Section 9 cites additional publications in both ESD and related areas.

Most of the work that has been published in connection with actual ESD is related to discharges from humans, usually grasping or in association with a metal object. Far less published data exists for discharges from humans without metal objects, and from mobile furnishings, and virtually no data exists for discharges from human torsos or clothing. For this reason, primary emphasis is placed on discharges from humans with associated metal objects, with some additional material relating to ESDs from mobile furnishings. All discharges are assumed to take place in an air environment.

Finally, all of the published time-domain data on which this guide relies were taken using instrumentation with either a 400 MHz or a 1 GHz bandwidth.

---

[1]The numbers in brackets correspond to those of the references in Section 3, and the numbers preceded by the letter "B" in brackets correspond to those of the bibliography in Section 9.

2. Definitions

antistatic. A property of materials that resist triboelectric charging.

approach speed. The rate at which the intruder approaches the receptor.

body/finger ESD. An electrostatic discharge from an intruding human finger or hand. Also called body/finger discharge.

body/metal discharge. See **hand/metal ESD**.

body/metal ESD. See **hand/metal ESD**. *Syn*: body/metal discharge.

brush-by. An electrostatic discharge from the human torso, such as from the hip or shoulder. *Syn*: brush-by ESD, brush-by discharge.

brush-by discharge. See **brush-by**.

brush-by ESD. See **brush-by**.

charge voltage. The voltage difference between the intruder and the receptor just prior to an ESD.

DES. Discharge Electrostatic; an alternative name for ESD.

direct ESD event. An ESD event that takes place between an intruder and a receptor in which the intruder or the receptor, or both, is an equipment victim.

equipment victim. The electronic equipment or subassembly that is subjected to the effects associated with an ESD event. It may be the intruder or receptor, or it may be in proximity to the discharge between the intruder and receptor and therefore subjected to the stress of ESD-related electromagnetic fields.

ESD. Electrostatic Discharge: the sudden transfer of charge between bodies of differing electrostatic potentials.

ESD current wave. The waveform of the discharge current between an intruder and a receptor.

ESD event. An interval that includes the ESD current, electromagnetic fields, and corona effects before and during an ESD.

fast approach. Approach speeds that engender short, subnanosecond risetime ESD current waves. Fast-approach speed depends on the voltage difference between the intruder and receptor, e.g., for rounded electrodes of 8 mm diameter, greater than 0.05 m/s, 1 m/s, and 10 m/s at charge voltages of 4 kV, 8 kV, and 16 kV respectively [13].

furniture ESD. An electrostatic discharge in which the intruder is an inanimate object such as a cart or chair, with or without a human in electrical contact with the object.

hand-to-metal impedance. The impedance between the human hand and the metal object with which it is associated in a hand/metal ESD. The metal object is usually the intruder discharge electrode. Examples of hand-to-metal impedance include resistance and capacitance

between the fingers and a key, between the wrist and a metal watch or bracelet, and between the hand and a screwdriver.

hand/metal discharge. See **hand/metal ESD**.

hand/metal ESD. An electrostatic discharge from an intruding human hand which occurs from an intervening metal object such as a ring, tool, key, etc. *Syn*: hand/metal discharge.

indirect ESD event. An ESD event taking place between an intruder and a receptor in proximity to equipment that is the victim.

initial current pulse. The subnanosecond risetime, and greater than 1 ns to perhaps 3 ns duration pulses that can occur at the start of the current wave from an ESD. Also called initial pulse, initial spike, and fast discharge mode. Its leading edge is the initial slope.

initial slope. The slope, in amperes per nanosecond (A/ns), that occurs at the start of the ESD current wave. *Syn*: rising slope.

intruder. The body that is in motion in an ESD event. The intruder is usually but not necessarily charged relative to its surroundings. It is always at a potential different from that of the receptor.

intruder electrode geometry. The size and shape of that surface of the intruder, termed the intruder electrode, at which the ESD takes place.

main discharge current wave. The relatively long portion of the ESD current wave that follows the initial current pulse, or that occurs by itself when the initial current pulse does not exist. It may be unidirectional or oscillatory; its initial slope may be fast or slow.

multiple ESD event. An ESD event in which more than one discharge occurs. The time interval between successive discharges may be several microseconds to several tens of milliseconds. Related terms include multiple ESD, multiple discharge, and multiple.

normalized peak ESD current. Ratio of the peak current to the charge voltage (e.g., 5A/kV).

normalized rising slope. Ratio of the initial slope to the charge voltage (e.g., 3.75 A/ns/kV).

proximity discharge. See **proximity ESD**.

proximity ESD. See **indirect ESD event**. *Syn*: proximity discharge.

receptor. The body that is at rest in an ESD event. The receptor is usually but not necessarily at the same potential as its surroundings. It is always at a potential different from that of the intruder.

receptor electrode geometry. The size and shape of that surface of the receptor, termed the receptor electrode, at which the ESD takes place.

rising slope. See **initial slope**.

SED. Static Electric Discharge; an alternate name for ESD.

static dissipative. Having a level of resistivity that typically leads to charge dissipation. (See Table 1.)

triboelectric charging. The generation of electrostatic charges when two pieces of material are brought into intimate contact and are then separated. *Syn*: triboelectrification.

triboelectric series. A list of substances in an order of relative positive to negative charging as a result of the triboelectric charging effect. (See Appendix A.)

triboelectrification. See **triboelectric charging**.

3. References

This standard shall be used in conjunction with the following publications:

3.1 Standards Publications

[1] ECMA TR-40, Electrostatic Discharge Immunity Testing of Information Technology Equipment, 1987.[2]

[2] EIA 571 (March 1991), Environmental Considerations for Telephone Terminals.[3]

[3] IEC Pub 801-2 (1991), Electromagnetic compatibility for industrial process measurement and control equipment. Part 2: Electrostatic discharge requirements.[4]

[4] MIL-STD 883D, Test Methods and Procedures for Microelectronics.[5]

[5] NEMA, "Environmental Testing for Electronic Controls—Residential Controls," Part DC-33, Draft proposed June 24–25, 1982.

[6] SAE J1113 (Aug. 1987), Electromagnetic Susceptibility Measurement Procedures for Vehicle Components (Except Aircraft).[6]

[7] UL 991-1989, The Standard Test for Safety-Related Controls Employing Solid-State Devices.[7]

3.2 Other References

[8] AT&T Technologies, *Electrostatic Discharge Control Handbook*, Issue 3, 1990.

---

[2]ECMA publications are available from ECMA, 114 Rue du Rhone, CH-1204, Genève, Switzerland/Suisse. ECMA publications are also available in the United States from the Sales Department, American National Standards Institute, 11 West 42nd Street, 13th Floor, New York, NY 10036, USA.

[3]EIA publications are available from Global Engineering, 1990 M Street NW, Suite 400, Washington, DC, 20036, USA.

[4]IEC publications are available from IEC Sales Department, Case Postale 131, 3 rue de Varembé, CH-1211, Genève 20, Switzerland/Suisse. IEC publications are also available in the United States from the Sales Department, American National Standards Institute, 11 West 42nd Street, 13th Floor, New York, NY 10036, USA.

[5]MIL publications are available from the Director, U.S. Navy Publications and Printing Service, Eastern Division, 700 Robbins Avenue, Philadelphia, PA 19111, USA.

[6]SAE publications are available from SAE, Customer Sales, 400 Commonwealth Drive, Warrendale, PA 15096, USA.

[7]UL publications are available from Underwriters Laboratories, Inc., 333 Pfingsten Road, Northbrook, IL 60062-2096, USA.

[9] Boxleitner, W., *Electrostatic Discharge and Electronic Equipment: A Practical Guide for Designing to Prevent ESD Problems*. New York: IEEE Press, 1989.

[10] Boxleitner, W., "Frequency of Occurrence of ESD to Information Processing Equipment," *EMC Expo Symposium Record*, pp. C1.26–C1.30, 1989.

[11] Byrne, W., "Development of an Electrostatic Discharge Model for Electronic Systems," in *Proceedings of the IEEE International Symposium on EMC*, pp. 199–205, 1982.

[12] Byrne, W., "The Meaning of Electrostatic Discharge (ESD) in Relation to Human Body Characteristics and Electronic Equipment," in *IEEE International Symposium on EMC,* pp. 369–380, 1983.

[13] Daout, B., Ryser, H., Germond, A., and Zweiacker, P., "The Correlation of Rising Slope and Speed of Approach in ESD Tests," in *Proceedings of the 7th EMC Symposium*, pp. 461–466, 1987.

[14] Daout, B. and Ryser, H., "Fast Discharge Mode in ESD Testing," in *Proceedings of the 6th EMC Symposium*, pp. 41-46, 1985.

[15] Daout, B. and Ryser, H., "The Reproducibility of the Rising Slope in ESD Testing," in *Proceedings of the IEEE International Symposium on EMC*, pp. 456–474, 1986.

[16] Gallagher, T. J. and Pearmain, A. J., *High Voltage Measurement, Testing and Design*. New York: John Wiley & Sons, 1983, p. 54.

[17] Greason, W. D., "Influence of a Ground Plane on the ESD Event in Electronic Systems," in *Proceedings of the IEEE/IAS Conference*, pp. 1658–1667, 1987.

[18] Honda, M. and Kowamura, R., "EMI Characteristics of ESD in a Small Air Gap," in *Proceedings of the EOS/ESD Symposium EOS-6*, pp. 124–130, 1984.

[19] Honda, M. and Ogura, K., "Electrostatic Spark Discharges: Three Factors are Critical," in *Proceedings of the EOS/ESD Symposium EOS-7*, pp. 149–154, 1985.

[20] Hyatt, H. and Mellberg, H., "Bringing ESD Testing into the 20th Century," in *Proceedings of the IEEE International Symposium on EMC*, pp. 220–225, 1982.

[21] Hyatt, H. C. and Mellberg, H., "A Closer Look at the Human ESD Event," in *Proceedings of the EOS/ESD Symposium EOS-3*, pp. 1–8, 1981.

[22] King, W. M. and Reynolds, D., "Personnel Electrostatic Discharge: Impulse Waveforms Resulting from ESD of Humans Directly and Through Small Hand-Held Metallic Objects Intervening in the Discharge Path," in *Proceedings of the IEEE International Symposium on EMC*, pp. 577–590, 1981.

[23] King, W. M. and Reynolds, D., "Personnel Electrostatic Discharge: Impulse Waveforms Resulting from ESD of Humans Through Metallic-Mobile Furnishings Intervening in the Discharge Path," in *Proceedings of the IEEE International Symposium on EMC*, pp. 212–219, 1982.

[24] King, W. M., "Dynamic Waveform Characteristics of Personnel Electrostatic Discharge," in *Proceedings of the EOS/ESD Symposium EOS-1*, pp. 78–87, 1979.

[25] McFarland, W. Y., "The Economic Benefits of an Effective ESD Awareness and Control Program—An Empirical Analysis," in *Proceedings of the EOS/ESD Symposium EOS-3*, pp. 28–33, 1981.

[26] Richman, P., "Classification of ESD Hand/Metal Current Waves Versus Approach Speed, Voltage, Electrode Geometry and Humidity," in *Proceedings of the IEEE International Symposium on EMC*, pp. 451–458, 1986.

[27] Richman, P., "Comparing Computer Models to Measured ESD Events," in *Proceedings of the EOE (Electrical Overstress Exposition)*, pp. 110–114, 1985.

[28] Richman, P., "Computer Modeling the Effects of Oscilloscope Bandwidth on ESD Waveforms Including Arc Oscillations," in *Proceedings of the IEEE International Symposium on EMC*, pp. 238–245, 1985.

[29] Richman, P., "The Effects of Hand-Associated Metal Object Geometry and Hand-to-Object Coupling Impedance on ESD Current Waves," in *Proceedings of the 7th EMC Symposium*, pp. 467–472, 1987.

[30] Richman, P., "An ESD Circuit Model with Initial Spikes to Duplicate Discharges from Hands with Metal Objects," *EMC Technology*, vol. 4, no. 2, pp. 53–59, Apr.–Jul. 1985.

[31] Richman, P. and Tasker, A., "ESD Testing: The Interface Between Simulator and Equipment Under Test," in *Proceedings of the 6th EMC Symposium*, pp. 25–30, 1985.

[32] Simonic, R. B., "Electrostatic Furniture Discharge Event Rates for Metallic-Covered, Floor- Standing Information Processing Machines," in *Proceedings of the IEEE International Symposium on EMC*, pp. 191–198, 1982.

[33] Speakman, T. S., "A Model for the Failure of Bipolar Silicon Integrated Circuits Subjected to Electrostatic Discharge," *12th Annual Proceedings of Reliability Physics*, pp. 60–69, 1974.

[34] Storm, D. C., "Controlling Electrostatic Problems in the Fabrication and Handling of Spacecraft Hardware," in *Proceedings of the EOS/ESD Symposium EOS-1*, pp. 4–6, 1979.

[35] Tasker, A., "ESD Discharge Waveform Measurement, the First Step in Human ESD Simulation," in *Proceedings of the IEEE International Symposium on EMC*, pp. 246–250, 1985.

[36] Tucker, T. J., "Spark Initiation Requirements of a Secondary Explosive," *Annals of the New York Academy of Sciences*, vol. 152, pp. 643–653, 1968.

[37] Weil, G., "Making Accurate and Repeatable Measurements of the ESD Current Waveform in the Regime of 1 GHz and Above," in *Proceedings of the 8th EMC Symposium*, pp. 355–360, 1989.

[38] Wilson, P. F., Ondrejka, A. R., Ma, M. T., and Ladbury, J. M., "Electromagnetic Fields Radiated from Electrostatic Discharges, Theory and Experiment," NBS Technical Note 1314, Feb. 1988.

4. Principal Methods of Charging Humans and Mobile Objects

Static electrification or charging refers to all processes that produce segregation of positive and negative electrical charges into relatively stationary groupings. This section describes

those processes considered directly relevant to the purposes of this guide. Supplemental information is given in Appendix A.

4.1 Triboelectric Charging. The most common charging mechanism is triboelectric charging. This mechanism involves electron or ion transfer upon contact, due to the frictional localized heating of microscopic contact areas on solid surfaces. The localized microscopic regions of material are melted, allowing increased charge mobility.

Distinctions among various levels of material resistivity are based on surface and volume resistance. Categories with corresponding ranges of surface and volume resistivity are given in Table 1. The electrostatic charge that can be developed between two materials is a function of their relative position in the triboelectric series, and of their resistivity. Those materials in the series that also have a higher resistivity can accumulate significant charge because a longer time is required for charge to bleed off such materials. However, under certain circumstances even conductive materials, such as metals, can be charged (see Table A1).

Table 1
Resistivity Classification for Purposes of Electrostatic Discharge

Classification	Surface Resistivity (Ω per square)	Volume Resistivity (Ω cm)
Conductive	$< 10^5$	$< 10^4$
Static-Dissipative	$10^5 - < 10^{12}$	$10^4 - < 10^{11}$
Nonconductive	$\geq 10^{12}$	$\geq 10^{11}$

4.2 Induction. Induction, or electrostatic induction, is a means by which portions of humans or other items can become differentially charged.

Such charge redistribution takes place on a body when the electrostatic field of a nearby charged object, such as the face of a cathode ray tube, polarizes charges of a nonconductive body or redistributes charges on a conductive body. As a result, even though the person or object as a whole may remain electrically neutral, its charge may be distributed unequally, thereby creating the possibility of an electrostatic discharge from some portion of the person or object.

4.3 Physical Charge Transfer. This type of charging occurs when charged particles are physically transferred to an object that is itself not creating the charge. For example, a person who is pushing an equipment cart, which is accumulating charge due to rolling friction, may be charged by the cart. Also, charging via an ion stream is another example of physical charge transfer.

4.4 Examples of Common Charging Processes

4.4.1 Motion, Walking, and Friction. One of the most common methods of charging is the act of walking. The human body, in the process of walking, builds up electrical charge with respect to its surroundings. Walking on a floor with footwear of an insulating material leads to charge buildup on the underside of the shoe sole by triboelectrification. The charged shoe soles cause charge redistribution on the human body by induction. As each step is taken, this charge redistribution increases. The maximum total electrostatic charge that can accumulate is on the order of microcoulombs, and significant electrostatic potentials can thus be devel-

oped. For example, walking across a synthetic fiber carpet in a relatively dry room (less than about 30% relative humidity) can easily result in an electrostatic potential from several kilovolts to over 10 kV. (See 5.2). Walking across many other floor coverings can also produce an electrostatic charge. In addition, waxing a floor may worsen the situation, thus adding to the electrostatic charge that may be developed. Rolling mobile furnishings, including chairs and carts, can also lead to charge buildup due to contact between the rollers and the floor. Other friction- based charging methods exist. For example, the simple movement of the body within clothing can develop large electrostatic potentials.

4.4.2 Ion-Generation Imbalance. Ionizers are often used to reduce the tendency of materials to build up or store electrostatic charge. However, if the ionizing equipment does not produce both positive and negative ions more-or-less equally, the ion stream may actually charge objects in its path. The electrostatic charging in this situation is not eliminated and may, in fact, be intensified.

4.4.3 Cathode Ray Tubes (CRTs). CRTs are used as display devices and sometimes as input devices (e.g., touch screens) for computer terminals, oscilloscopes, and television sets. They can be sources of charge because they involve a beam of electrons accelerated by a high internal voltage. It is typically the field surrounding the screen that can charge humans and nearby objects, including other portions of the CRT assembly, because charges may be redistributed on objects near, but not touching, the CRT. (See 4.2.) However, if a person or a small mobile furnishing should physically contact the CRT, a portion of the CRT charge may be transferred to the person or object. (See 4.3.)

4.4.4 Additional Triboelectric Charging Methods. Any frictional contact between materials can lead to electrostatic charging of personnel and/or mobile furnishings. The tendency to charge is maximized as the electrical dissimilarity between contacting surfaces is increased, humidity reduced, and kinetics of contact become more violent. For example, driving belts are often significantly charged during their movement, as is adhesive tape when it is removed from a dispenser. Personnel or furnishings in contact with such charged items may therefore have significant charge induced.

5. Charge Accumulation: Characteristics and Variables

The static charge that can be accumulated by an object is influenced not only by the physical characteristics of the object itself, but also by the environment in which the object is located.

5.1 Charge. The electrostatic potential or potential difference that exists between two charged objects, or between a charged and an uncharged object, may be considered to exist between two electrodes of a charged capacitor, where the objects represent the capacitor electrodes. The charge Q, expressed in coulombs, is related to the capacitance and voltage by the equation:

$$Q = CV \qquad \text{(Eq 1)}$$

where

C = Capacitance (in farads)
V = Voltage (in volts)

The values of C and V depend upon the composition and geometry of the materials and the environment. Depending upon the exact physical and environmental conditions, the charge

may range from a fraction of a microcoulomb to several microcoulombs. The geometry of the surface of a charged object limits the surface charge density and the electric field intensity associated with it. For a given electrostatic charge on a body, charge density is greater at sharp edges or corners. The corona discharge voltage, approximately 3×10^6 V/m, limits the amount of charge that an object can sustain [12].

Consider the example of a person walking across a carpet and becoming charged to 10 kV. Assuming a body capacitance of 100 pF, the charge the person carries may be calculated as $Q = CV = [100 \times 10^{-12}] [10 \times 10^3] = 1\ \mu C$.

5.2 Electrostatic Potential. The voltage that is developed on both human bodies and on mobile objects, with respect to local electrostatic ground potential, is a strong function of a number of environmental variables. Foremost among them are relative humidity and the materials of floor coverings, clothing, etc. High relative humidity increases the conductivity of many materials and thus permits charge to drain from the object, lowering the maximum achievable electrostatic potential. Conversely, low relative humidity allows an object to achieve a relatively high electrostatic potential. Nonconductive materials will retain a charge almost indefinitely while static-dissipative and conductive materials permit charge to drain off.

The voltage on a human body or on a mobile object can therefore vary widely from one environment to another. It can remain well below 5 kV in controlled humidity situations involving only antistatic or static dissipative materials. It can range from 5 kV to over 10 kV in low humidity environments with synthetic materials.

The general expression relating Q, C, and V, i.e., $Q = CV$, indicates that if the capacitance of a body is reduced, its voltage must increase as long as its charge does not change. This occurs, for example, when a seated person elevates his or her feet, e.g., placing them on a cross-member under a table. The resulting reduction in body capacitance with reference to earth causes a multiplication of the voltage carried just prior to lifting the feet. The voltage multiplication factor can be 1.5 or even higher in extreme cases.

Finally, it has been claimed that charge voltage can be as high as 20 kV to 25 kV when both extremely low humidity environments—below 20% to 30% relative humidity—and nonconductive synthetic materials are involved [11], [25], [33], [34]. An ultimate limit for such extreme environments would be 30 kV to 40kV, at which voltage levels corona would bleed off charge via rings, watches, and other sharp points on the human body or mobile object [11]. However, more recent work may put some of these extremely high-charge voltages in question; at issue is the inaccuracy of some charge meters when the charged object is as large as the human body.

The minimum voltage necessary for a person to be aware of his or her involvement in an electrostatic discharge is approximately 3000 V. Nevertheless, electrostatic discharges that occur below this threshold of human perception may contain sufficient energy to cause upset or damage to electronic equipment. In fact, the faster initial slopes of current waveforms that result from ESD events at these low voltage levels can make such discharges even more disruptive than ESD events originating at higher charge voltages. (See 7.2.)

5.3 Capacitance. The capacitance of an object with reference to its surroundings is directly proportional to the size of the object and is a function of the proximity and characteristics of the surroundings. The shape or geometry of the object also affects its capacitance. A body with no nearby surroundings still has capacitance to free space. There is typically only a small difference between capacitance to free space and capacitance to objects more than a meter away.

As an example, effective human body capacitance is on the order of 60 pF to 300 pF. The range of variation includes not only size and geometry, but proximity to grounded surfaces or objects and the dielectric constant of the intervening material(s), e.g., air and shoe sole material.

5.4 Energy. The energy stored on a human body or mobile object is a function of its capacitance and its voltage and is determined by the relationship:

$$W = (1/2)\, CV^2 \qquad \text{(Eq 2)}$$

where

C = Capacitance (in farads)
V = Voltage (in volts)
W = Energy (in joules)

As an example, consider a person walking across a carpet and becoming charged to 10 kV. Assuming a body capacitance of 100 pF, the stored energy would be determined as $W = (1/2)CV^2 = [1/2]\ [100 \times 10^{-12}]\ [10 \times 10^3]^2 = 5$ mJ.

5.5 Environmental Factors. Variables such as relative humidity; temperature; atmospheric pressure; materials; contaminants; object shapes; and the proximity of the intruder, the receptor, and the equipment victim will control the charge that is developed on the bodies with respect to each other and with respect to local electrostatic ground. Of all these variables, materials and relative humidity are prime factors in determining the relative ease with which objects will become charged to a given voltage.

In addition, the geometry of the object surfaces, as well as object spacings, affect charge density and electric field intensity. All of these factors must be considered when evaluating an electrostatic environment.

6. ESD: Characteristics and Variables

6.1 Intruders, Receptors, and Equipment Victims. The intruder is often a human hand, with or without an associated metal object such as a key, ring, or tool. But it may be any object such as a chair, an equipment cart, a vacuum cleaner, etc.

The receptor is the stationary object that the intruder approaches and to or from which it transfers charge. Often the receptor is at local electrostatic ground potential.

The equipment victim is an electronic device that is often the receptor, but may also be the intruder or an object that is neither the intruder nor the receptor. In this last case, the equipment victim is in close proximity to the ESD event and may be upset or damaged by the electromagnetic fields generated by the discharge between the intruder and the receptor.

When either the intruder or the receptor is an equipment victim, the ESD is termed direct. When the equipment victim is neither the intruder nor the receptor, the ESD is termed indirect.

Fig 1 shows a direct ESD event. The intruder may be human (Figs 2 and 4), inanimate (Fig 8), or a combination of the two (Figs 3, 6, and 7).

Table 2 lists the various kinds of intruders, with the names of the ESD events that result from each.

In the case of a human intruder, the ESD event may be a body/finger ESD that takes place directly from the skin (Fig 2). It may also be a brush-by that takes place from the torso (Fig 4) [12].

In the case of a human in contact with a small metallic object, a body/metal or hand/metal ESD is one that takes place from a metallic object associated with a hand such as a ring, watch, screwdriver, or key (Fig 3). If the human is not in conductive contact with the small metallic object, the source of the ESD charge is only the metallic object (Fig 8).

In the case of a large inanimate intruder, the ESD event is called a furniture ESD and takes place from a specific conductive location on the intruder. Inanimate intruders include equipment carts without a human (Fig 5), with a human (Fig 6), and chairs (Fig 7).

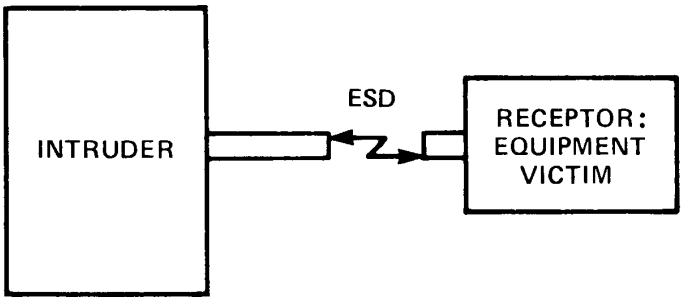

Fig 1
Direct ESD Event

Table 2
ESD Intruders and Resulting ESD

ESD Intruder	Type of Resulting ESD
Human	*Body/Finger*—from finger without associated metal object
	Brush-By—from hip, torso, or shoulder
Metal object	*Hand-Associated*—tool or other object not in conductive contact with the hand or body
	Furniture—not in conductive contact with the hand or body
Combination human and metal object	*Body/Metal or Hand/Metal*—tool, ring, watch, or other metal object in conductive contact with the hand or body
	Furniture and Human—in conductive contact with the hand or body; human seated in chair, pushing cart, or vacuum cleaner; holding and in conductive contact with a tool, etc.

The energy transferred from an intruder to a receptor during an ESD depends on the impedance ratio between them and on the energy dissipated in the arc.

Fig 9 shows an indirect ESD event. The equipment victim is irradiated by fields from three principal sources as a result of the electrostatic discharge: the ESD arc, the intruder mass, and the receptor mass. Additional sources include wires and cables that may be connected to the intruder or to the receptor, and reflections from adjacent objects and walls. All of these fields may affect the equipment victim.

6.2 Conditions Affecting Discharge Current. Just as the environment affects the charging process, it also affects the discharge current. Humidity, atmospheric pressure, and electrode shapes will affect the discharge current wave. In addition, the speed at which the intruder approaches the receptor is important. A rapid approach will result in a discharge current with a faster initial risetime than for a slow approach [13], [26]. (See B1 and B2).

As mentioned in 5.3, the capacitance of both intruder and receptor are dependent on adjacent ground structures. Therefore, the presence of such structures will also impact the discharge current [17].

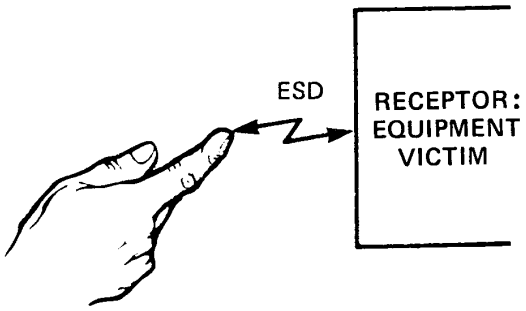

Fig 2
Direct Body/Finger ESD

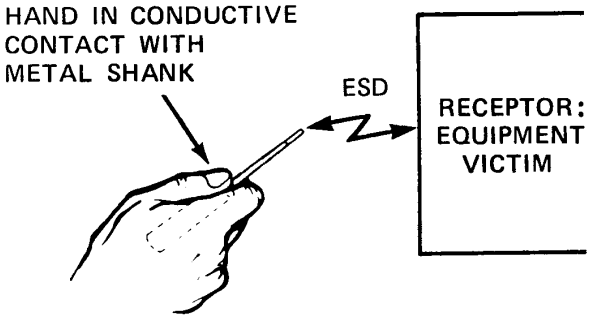

Fig 3
Direct Hand/Metal ESD or Body Metal ESD

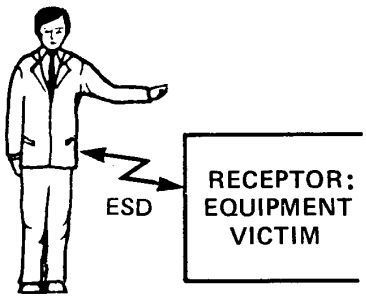

Fig 4
Direct Brush-By ESD

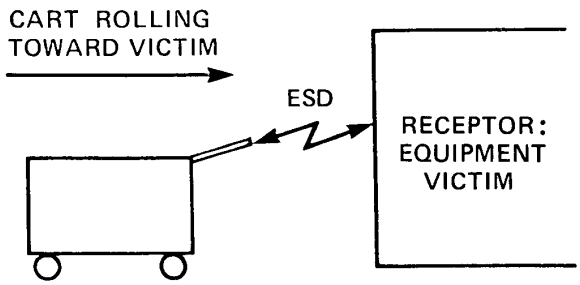

Fig 5
Direct Furniture ESD: Rolling Cart Alone

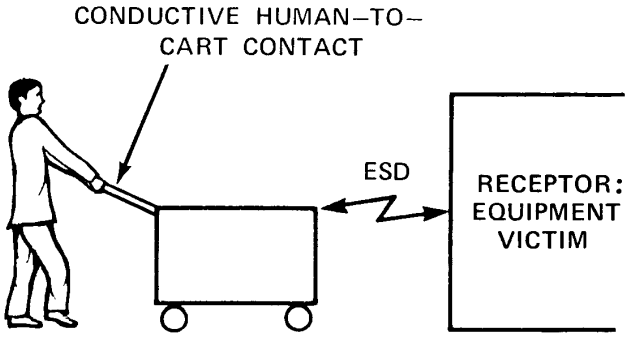

Fig 6
Direct Furniture ESD: Rolling Cart With Human

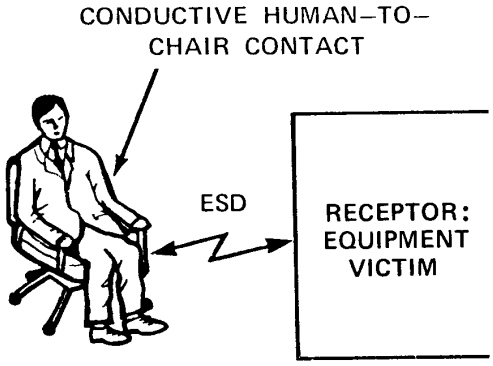

Fig 7
Direct Furniture ESD: Rolling Chair With Human

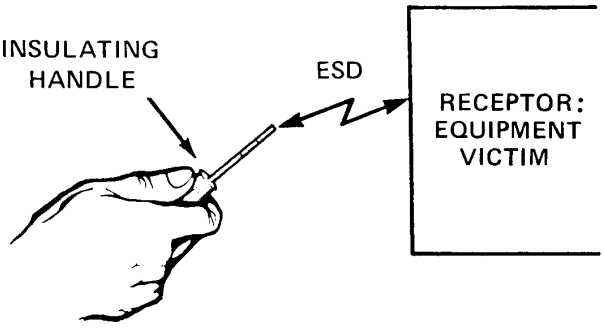

Fig 8
Direct Furniture ESD: Screwdriver Alone

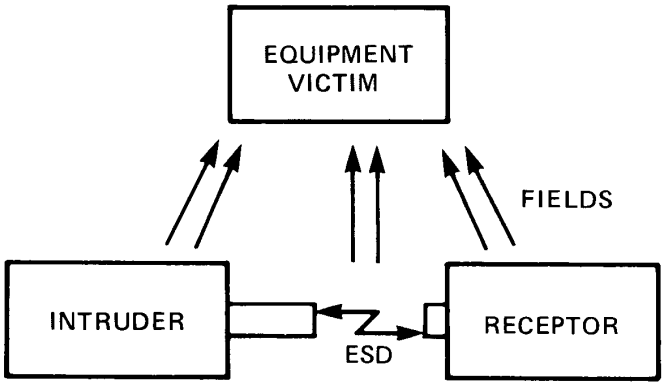

Fig 9
Indirect ESD Event

6.3 Frequency of Occurrence of ESD. The primary source of ESD incidence information is a 1.3 year study of metallic-covered, floor-standing, information processing equipment [32]. This equipment was installed at several different locations. Some locations were computer rooms, in which an attempt was made to control ESD by maintaining high relative humidity (the mean relative humidity was 31% to 43% for these sites) by using special carpets, etc. Other locations were offices in which no special effort was made to control ESD.

Current monitors were installed in order to detect ESD current in equipment. The detected current pulses were recorded and grouped by amplitude (see Fig 10). In this way a record was created that indicated the frequency of incidence of various ESD current amplitudes.

The limits of the current ranges in Fig 10 are the maximum that may be expected in an uncontrolled environment. In a controlled environment, high current levels may not occur. The maximum level in a controlled environment will depend on the effectiveness of the control methods used. For example, the study indicates that the occurrence of ESD is not related to humidity in a linear manner. As the relative humidity is reduced from 50% to 5%, the rate of ESD occurrence was found to increase nearly 100 times.

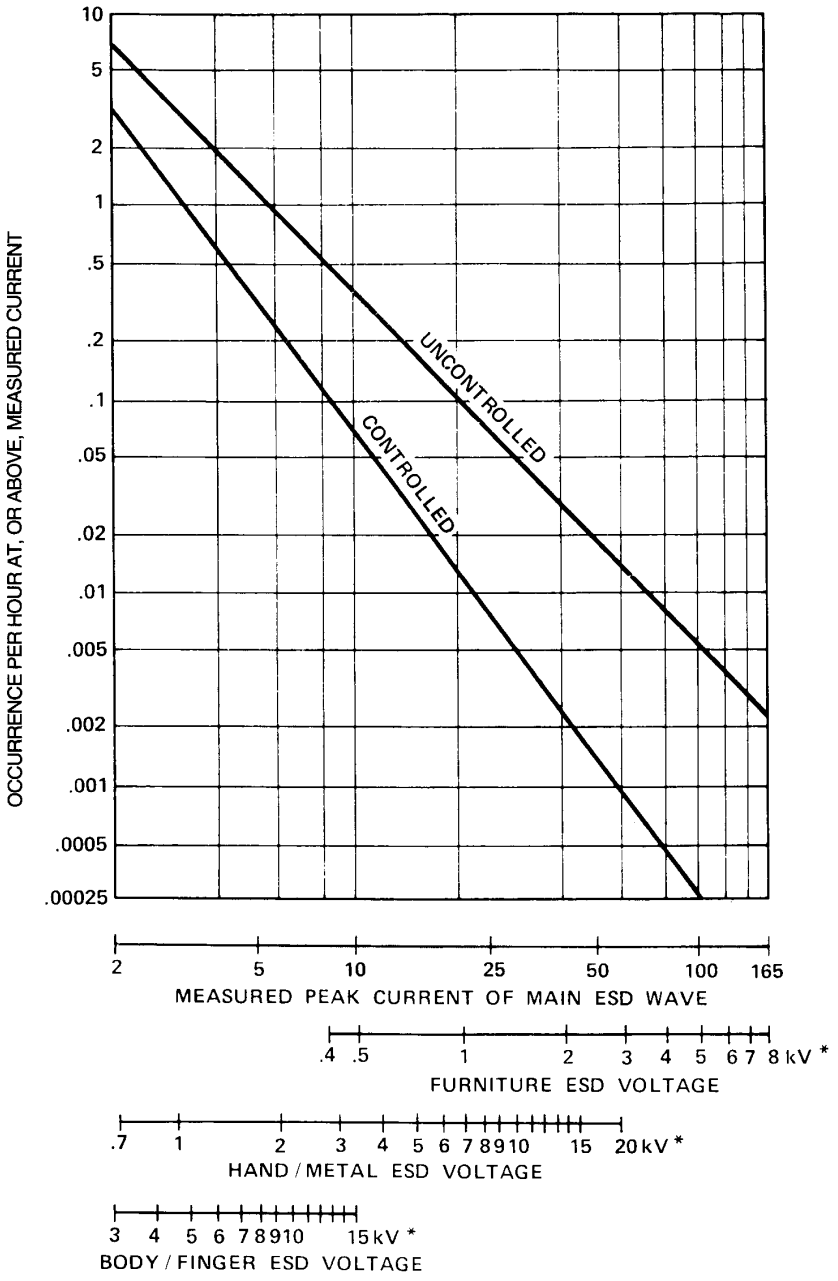

Fig 10
Average ESD Occurrence Per Equipment Victim

*In each specific controlled environment, the actual maximum charge voltage may well be much less than these limits. The actual limits will depend on the success of the control methods employed.

The bandwidth of the current monitor was 100 MHz. Since ESD current bandwidth can extend beyond 1 GHz, this would appear to cast doubt on the results of the study. However, this was not actually a problem. A 100 MHz current monitor can measure current pulses with a rise time of 3.5 ns. This is sufficient to determine the peak amplitude of the main discharge current wave in an ESD (see 6.4.2). Measurements of ESD currents indicate that the peak amplitude of the main discharge current wave is roughly proportional to the ESD charge voltage for a given intruder and receptor. Using the measured peak current, the charge voltage may be calculated using the equation $V = IZ$, where Z is the impedance of the ESD current path.

6.3.1 Occurrence of Personnel and Furniture ESD. An impedance based on furniture ESD was used to calculate the voltage scale (specifically 48 Ω). This impedance included the average impedance of the charged furniture, the ESD arc, and the path to the current monitor (see Fig 10) [10].

Since most equipment designers are usually interested in human ESD as well as furniture ESD, Fig 10 also has charge voltage scales for body/finger ESD and for hand/metal ESD. The impedance used to relate the body/finger ESD current to the charge voltage was 1500 Ω.

Although 1500 Ω is somewhat higher than the lowest theoretical human body impedance [12], measurement of actual human ESD events indicate that 1500 Ω should be considered a reasonable worst-case impedance for body/finger ESD. Therefore, this value is the human body impedance used in UL and MIL standards [4], [7].

For the hand/metal ESD scales in Fig 10, the impedance used to calculate the charge voltage was 330 Ω. This value was chosen because measurement of actual hand/metal ESD indicates that this is a reasonable worst-case impedance, and it therefore is used in several test standards [1], [3], [B1].

Of course, in the real world the impedances of ESD discharge paths will vary. For all three types of ESD, the impedance could easily be at least a factor of two different from the impedances used to develop the voltage scales of Fig 10. Therefore, the voltage scales shown in Fig 10 are not to be considered precise. In addition, the ESD current measurements that form the basis for Fig 10 represent an average over many sites, and variation from site-to-site can be much larger than a factor of 2. In spite of these limitations, however, Fig 10 gives a useful indication of how often ESD will occur, on the average, at various charge voltages in both controlled and uncontrolled environments.

The three voltage scales of Fig 10 overlap. Since the study counted all types of ESD, it is not possible to say what the ratio of occurrence was for furniture ESD, hand/metal ESD, or body/finger ESD. Therefore, in the regions where the voltage scales overlap, it is only known that the number of ESDs events that occurred was due to a combination of the overlapping types of ESD.

6.4 General Characteristics of the ESD Event. It is the purpose of this section to establish common nomenclature to facilitate description and analysis of ESD events.

6.4.1 ESD Voltage Regions. All of the current waves generated by ESD events fall into two general classes: those with, and those without, an extremely steep initial slope.

The current wave from a human ESD often includes an initial spike preceding the main discharge wave; such an initial spike usually has a steep initial slope. The current wave from furniture ESD may not include an initial spike, yet often has a steep initial slope. The ESD current waves that include such steep initial slopes often have rise times that are so fast that, when 1 GHz bandwidth instrumentation is used, the rise times are displayed as the instrumentation's own, namely 350 ps. It is presumed that when wider bandwidth instrumentation is available, ESD rise times may be shown to be even faster. B1 and B2 give additional background information on the initial pulse and on the conditions that may determine whether or not an initial pulse is generated in a particular ESD. B1 also includes information on the importance of a steep initial slope on equipment failure probabilities.

Those ESD current waves that do not have a steep initial slopes have rise times ranging from one or several nanoseconds to tens of nanoseconds; typical values lie between 2 ns and 20 ns.

Three different ESD voltage regions are defined, as shown in Fig 11:

Region I: From 0 V to 3–4 kV. The typical ESD current wave is repeatable, and it has an initial slope with a rise time of greater than 1 ns. Human ESD in this region almost always has an initial current pulse; ESD-generated fields also typically have initial slopes with rise times greater than 1 ns, but field wave data in the technical literature is limited at this time.

Region II: From 3–4 kV to 8–10 kV. This transition region is intermediate to regions I and III. In it, current wave repeatability becomes poor. A steep initial slope and an initial current pulse can appear and disappear from one ESD event to the next, under apparently invariant test conditions. Thus, region II starts where rise time varies and the initial current pulse may not appear for human ESD, and ends where rise time is almost always relatively slow and the initial current pulse almost never appears. ESD current and field characteristics lie between those of regions I and III; waves are highly variable.

Region III: Above 8–10 kV. The ESD current wave has an initial slope with a relatively long, 2-30 ns rise time. The initial current pulse is absent, and current waves are often notched. ESD-generated fields also typically have initial slopes with 2-30 ns rise times, but field wave data in the technical literature is limited at this time.

It should be emphasized that while the voltage region representation permits some cataloging of ESD waveforms, in fact the voltage region system is not absolute. However, it does serve to introduce the manner in which current, rise time, and the existence of the initial current pulse depend on charge voltage, when all other conditions are equal. In fact, human ESD events with very fast rise times and initial current pulses can be produced at charge voltages over 10 kV for extremely fast approach speeds, particularly at low humidity [26]. By the same token, human ESD events with no initial current pulses, and with quite slow (2-30 ns) rise times, can be generated at only 1-2 kV, using supersharp metal objects and quite slow approach speeds, particularly at high humidity [26]. However, these are extremes. For classifying ESD current waves in terms of their basic characteristics, it is useful to define 3–4 kV and 8–10 kV demarcations between voltage regions as given above for typically rounded electrodes in medium speed approaches. Different points of demarcation may be established, when desired, for special purposes.

A discharge in region I is roughly equivalent to a switching operation, since the discharge is essentially free from the variability that may be introduced by corona and possibly by other effects at higher voltages. Therefore, tests with both human and furniture discharge can be extremely repeatable in this region; in some circumstances, successive current waves can almost overlay one another for reasonably constant test conditions [13], [26]. On the other hand, such repeatability is not characteristic of transition region II, or of the always slower rise time, no initial current pulse of region III. In both regions II and III, a high degree of variability exists in the discharge current waveform.

Because of the high variability in regions II and III, ESD models in this guide refer only to region I. The models may not be accurate for regions II and III, since the quantitative effects of corona or other effects have a very limited data base.

6.4.2 Time Domain Characterizations of the ESD Current Wave. In the time domain, ESD current waves depend on whether the ESD source is human or furniture. An additional consideration is whether conditions lead to generation of a steep initial slope and to the existence of an initial spike.

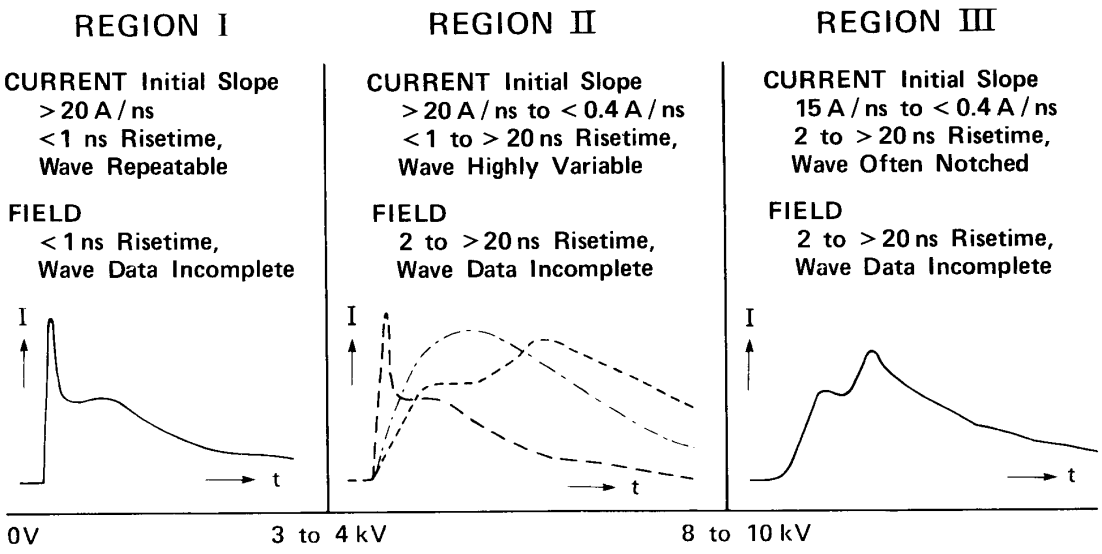

Fig 11
ESD Voltage Regions

NOTES: (1) Typical examples of current waveforms and field characteristics are shown for each region; amplitudes are normalized.
(2) Applicable for 3 mm to 10 mm diameter metal electrodes and typical approach speed (.02 m/s to .2 m/s).

ESD wave parameters that may be related to malfunction of electronic equipment, and are therefore of interest in ESD characterization, are:

— Initial slope of the current pulse (A/ns)
— Peak amplitudes of
  — The initial slope
  — The initial current pulse
  — The main discharge wave
— Amplitudes of the ESD current wave at specific time intervals after its start

The waveform and magnitude of the current that flows during charge transfer between the intruder and the receptor are critical factors in determining both the character and the level of the ESD threat to the equipment victim. In particular, ESD can be grouped into three voltage regions (see 6.4.1 and Fig 11). A complementary classification results from consideration of the type of discharge involved: body/finger, hand/metal, or furniture (see 6.1 and Table 2).

Body/finger and hand/metal ESD events generate similar discharge current waveshapes; however, those of hand/metal ESD are typically between five and ten times larger in magnitude than those of body/finger ESD [22]. Waveforms from furniture ESD are totally different both in character and in magnitude from both types of human discharge waves, due primarily to the far lower total circuit resistance and inductance of metal furniture versus the human body. However, it would appear that a fast furniture discharge rise time or initial slope may occur under the same general conditions—electrode shapes, approach speeds, charge volt-

ages—as are required for generation of the initial current pulse in a human ESD; in other words, the voltage region characterization of 6.4.1 appears to hold with equal validity. Although 6.4.1 indicates that waveforms can vary significantly, only four to six basic waveshapes are generally needed to cover all of the different possibilities [23], [26].

Fig 12 shows current waves for typical hand/metal ESD events. Fig 12(a) shows a wave from ESD taking place in what may be presumed to be voltage region I; it therefore has a steep initial slope and an initial spike. Fig 12(b) shows the leading edge of the wave of Fig 12(a), emphasizing the initial slope, the current range of the initial slope, and the peak of the initial current pulse.

Various points are identified in Fig 12(a), including the peak of the main discharge current wave and the peak amplitude of the initial spike. Also indicated are the values of the current at 30 ns and 60 ns after the start of the wave. These two points are recommended for specifying main discharge wave amplitude for hand/metal and body/finger ESD. The 50% point on the decay of the main discharge wave (not shown in the figure) is deprecated as an indicator of amplitude, since anomalies on the tail of the wave can be severe, depending on adjacent ground structures and other variables. In any case, it can often be difficult to determine the peak value of the main discharge wave since in many ESD events the initial spike overlies the main wave peak. The 30 ns and 60 ns points are less sensitive to such factors and are unambiguous; their use is therefore preferred.

Fig 12(c) shows a hand/metal ESD wave initiated from a higher charge voltage (or from a sharper point or slower approach). This wave displays a much slower initial slope and has no initial pulse, both of which characterize some ESD events in region II and virtually all ESD events in region III.

Fig 13 shows current waves from typical furniture ESD events. Fig 13(a) shows a wave from an ESD taking place in what presumably was region I. It therefore exhibits a steep initial slope, but it does not have an initial spike; initial spikes occur less frequently with furniture ESD events than with body/finger or hand/metal ESDs, even in the same voltage region. The main discharge wave for furniture ESD is typically oscillatory, since the total resistance in the discharge path is not much more than the ESD arc resistance, i.e., there is minimal damping in the circuit.

Fig 13(a) includes the peak of the main discharge wave (which is also the peak of the first half-cycle of the oscillation), the duration to the first axis crossing, and the amplitude of the first negative peak.

Fig 13(b) shows leading edge detail for the furniture discharge wave of Fig 13(a), emphasizing the initial slope and the current range of the initial slope. The peak of the initial current pulse is not shown since an initial current pulse has been assumed not to exist in this example. Note that the current range of the initial slope for furniture discharge may correspond fairly well with the peak of the initial spike for the hand/metal ESD. However, it is typically only 30% to 50% of the peak of the furniture ESD itself.

Fig 13(c) shows a wave from a furniture ESD initiated from a higher charge voltage (or from a sharper discharge point or slower approach), displaying the much slower rise time that is characteristic of some ESD events in region II and virtually all ESD events in region III.

Finally, Fig 14 shows an overlay of the typical waves of Figs 12(a) and 13(a) for region I hand/metal ESD and furniture ESD respectively. The initial slope portions of the two waves overlie one another, as these typical region I events may well do. After reaching the peak of the initial slope portion of the wave, the hand/metal wave drops and starts its much lower main discharge portion (shown later to depend on the discharge from the human body). The furniture wave, on the other hand, after reaching the peak of its initial slope, continues upward at a much slower rate to the peak, often twice as great as the current at the top of the initial slope portion. This is the first peak of the main furniture discharge wave oscillation, a function of the physical size of the main body of the furniture from which the ESD takes place. The almost identical initial slopes for hand/metal and furniture ESD events in region I, with vastly different main discharge waves following the initial slope, are explained in 6.5, describing models for the ESD event.

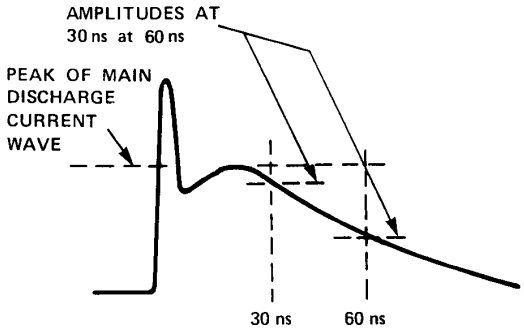

(a) Full Hand/Metal Wave

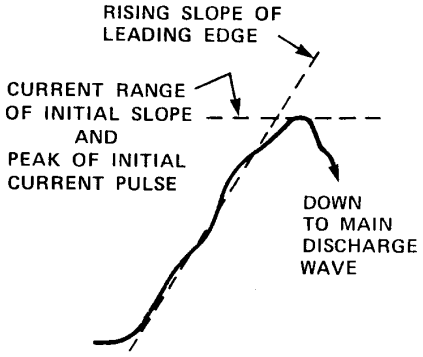

(b) Initial Slope of Hand/Metal Wave of (a)

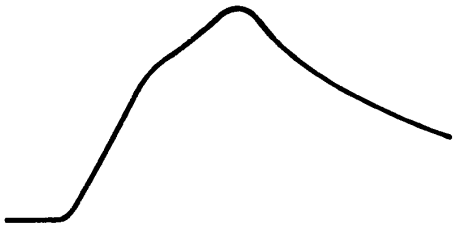

(c) Hand/Metal Wave Without Initial Spike

Fig 12
Hand/Metal ESD Current Waves

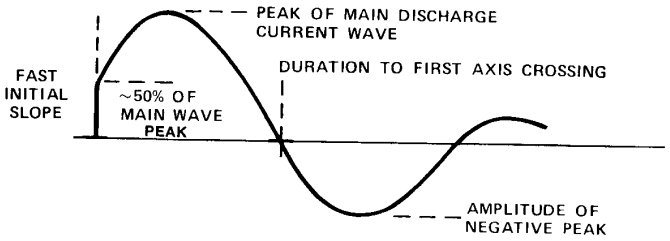

(a) Full Furniture Wave (Fast Front)

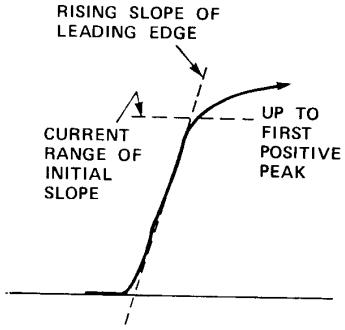

(b) Initial Slope of Furniture Wave of (a)

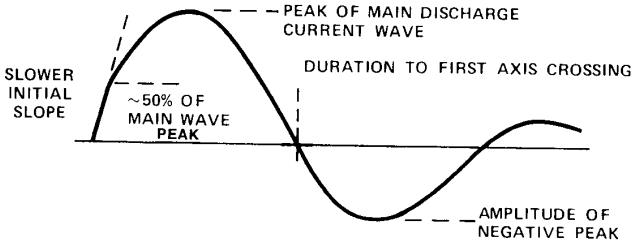

(c) Full Furniture Wave (Slow Front)

Fig 13
Furniture ESD Current Waves

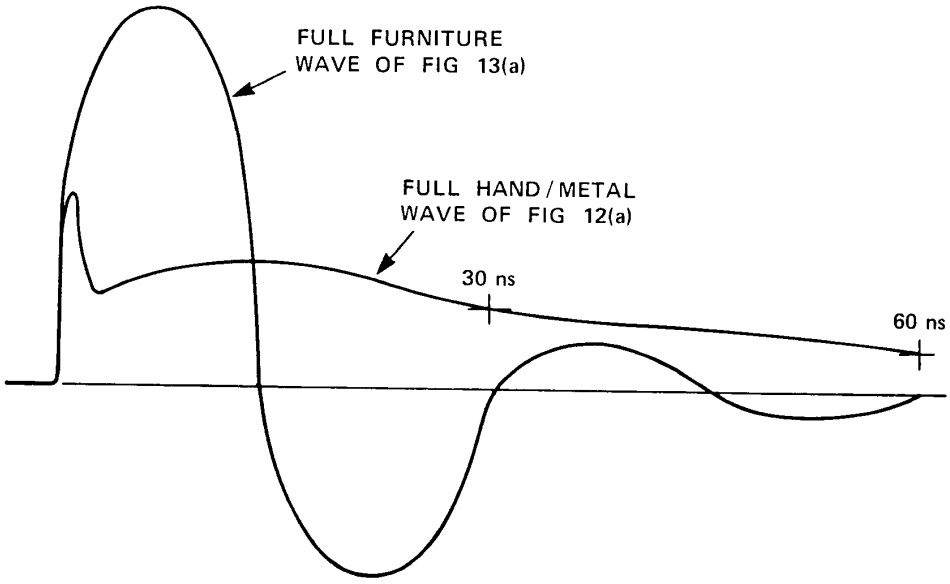

Fig 14
Overlaid Current Waves From Hand/Metal and Furniture ESD Current Waves

NOTE: Note the relative amplitudes and the common fast initial rise for the same charge voltage.

6.4.3 Spectra. The results of electromagnetic field measurements cited in 7.2 suggest that the slower current wave risetimes in voltage region III and in the upper portion of voltage region II are responsible for the limited energy above a few hundred megahertz for the spectra of ESD events in these regions [18], [19], [38].

Direct calculations for ESD current wave spectra indicate that ESD that include initial spikes may have spectral components that extend to several gigahertz [38].

6.4.4 Multiple Discharges. What is apparently a single ESD event may in fact incorporate more than one pulse of electromagnetic energy, taking the form of multiple pulses of current and associated electromagnetic fields. Multiple discharges are more likely to occur at higher charge voltages, above 10 kV or 12 kV; they are usually in a sequence of diminishing rise times [37]. The several pulses in a multiple ESD event are spaced by tens of microseconds to tens of milliseconds. Therefore, more than one theory has been developed to explain these phenomena (see B3). To date, no research has been reported to verify which of these theories are correct.

Since succeeding ESDs in a multiple discharge occur at descending charge voltage levels, many if not most high-voltage ESD events are accompanied, in multiples, by subsequent medium- and low-voltage ESD events. Therefore, the initial high-voltage ESD, which has a current waveform with a slow initial slope (see 6.4.1, 6.4.2, and 6.4.3), may be followed by one or more subsequent ESD events generated from lower charge voltages, which therefore often display steep initial slopes. In this way, a region III slow rise time ESD event may, via multiple discharge, also generate one or more region I fast initial slope ESD waveforms. This may

be one reason for the reappearance at high charge voltages, in region III, of equipment failures that occur at lower voltages, in region I, and sometimes disappear at medium voltages, in region II. The failures may simply be reappearing due to the fast rise time lower voltage ESD waveforms, which naturally follow many high-voltage discharges as a consequence of multiples. However, the total energy of the typical discharge current wave due to high voltage is also of course much greater than at lower voltage, and that may instead be the reason for the reappearance of equipment failures in region III. In fact, both explanations may be valid, each accounting for failure reappearance in different circumstances. The issue will remain an open question until additional work is performed and reported.

6.5 Electrical Models of the Direct ESD Event. The three sources of ESD that are of greatest interest to designers of electronic equipment, and that are therefore most important to model, are:

(1) *Body/Finger ESD:* Discharge from a fingertip without an associated metal object (Fig 2)
(2) *Body/Metal or Hand/Metal ESD:* Discharge from a metal object in contact with a hand (Fig 3)
(3) *Furniture or Inanimate Object ESD:* Discharge from a cart, chair, or other inanimate object, with or without a human in conductive contact with the object (Figs 5–8)

NOTE: Models are accurate only for voltage region I.

6.5.1 Simple Resistor Capacitor (RC) Model for Human ESD. The historical model of a human body ESD typically consisted of a simple series-connected resistor-capacitor network. This circuit is illustrated in Fig 15. Values contained in the literature for the capacitor range from 60–300 pF and, for the resistor, from 150–10 kΩ. [1], [2], [3], [4], [5], [6], [7], [12], [B1].

The historical model ignores the inductance of the human body, as well as the inductance inherent in any actual circuit that may be constructed to duplicate the model..

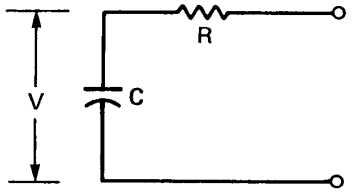

Fig 15
Simple RC Model for Human Body ESD

6.5.2 Developing a More Realistic ESD Model. Every portion of any object has a capacitance to free space, or to its surroundings, including other objects and portions thereof. Each object also has inductance between its capacitances and the point of electrostatic discharge.

The unique electrical characteristics of an ESD event result from interaction among the resistance, capacitance, and inductance parameters for all of the individual sections of every object, including humans, involved in the event. These electrical characteristics and their relationships may be used to construct an electrical model of the physical bodies involved in the discharge. The model is then useful in understanding currents and fields produced during the ESD event, and to assist in designing products and in developing standards for ESD immunity testing [9].

Fig 16 shows the capacitances involved in an ESD. Inductances and resistances are ignored in this simplified diagram since it is the capacitances that store the energy that is transferred

during an ESD event, and therefore their topology must be understood first. Those capacitances involved in the subnanosecond, discharge-current rise times are the ones associated with physical areas on the intruder and on the receptor that are closest to the points at which the discharge occurs.

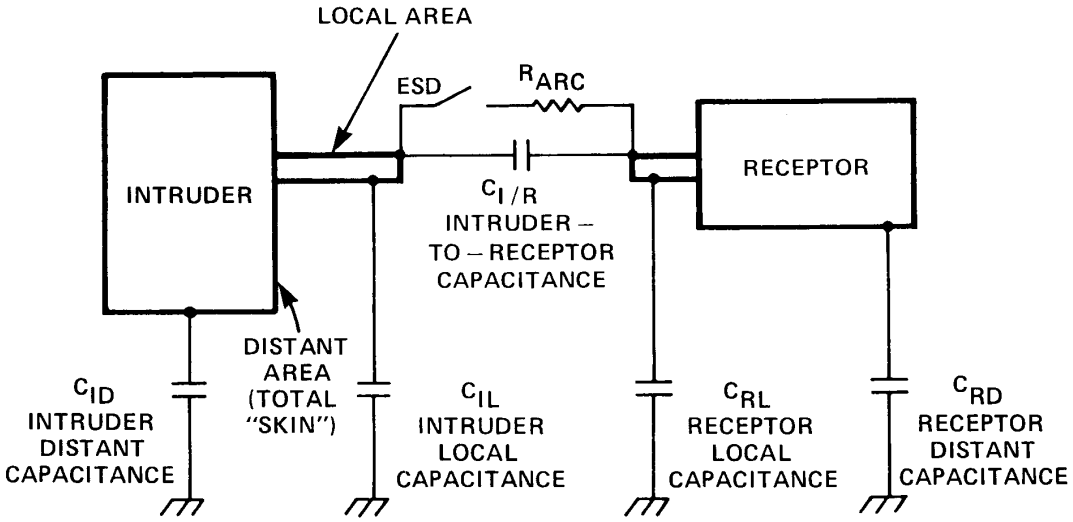

Fig 16
Capacitance Model for Participants in an ESD Event

Each of the local intruder and local receptor areas has capacitance to its surroundings, C_{IL} and C_{RL} respectively, in addition to the capacitance between the two areas $C_{I/R}$ (The subscript I refers to intruder, R to receptor, and L to area that is local with respect to the discharge.) Capacitances to the surroundings from areas on the intruder and receptor that are distant from the points of discharge are termed C_{ID} and C_{RD} respectively; these account for the longer duration and slower rise-time portions of the current wave. (The subscript D refers to area that is distant with respect to the discharge.)

Fig 17 shows the same circuit as Fig 16 except for the addition of inductance, and, where applicable, resistance, in series with each of the capacitors. Subscripts associate each inductance or resistance with its corresponding capacitance: L_{ID} with C_{ID}, etc.

Inductances must be included in realistic circuit models representing both the intruder and the receptor [9]. The initial slope of the current waveform, di/dt, is in fact determined not by the values of resistance and capacitance in the circuit model, but is proportional to the quotient of charge voltage divided by the total circuit inductance in the discharge path, or V/L [31]. Smaller objects, and small portions of larger objects in the immediate vicinity of the ESD, have geometries that generally result in low values of inductance. They can therefore produce discharge current waveforms with steep initial slopes in the subnanosecond range. The more distant portions of larger objects can generate greater peak currents, particularly if they are metal and therefore have very low equivalent series resistance. However, they will typically generate slower discharge current initial slopes, due to the higher inductances implied by greater distance from the point of discharge.

The three capacitances associated with areas close to the ESD, C_{IL}, $C_{I/R}$, and C_{RL}, are quite small. Typical values for each lie in the range of 3 pF to 20 pF. However, each of the three capacitors has extremely low series inductance; the total of L_{IL}, $L_{I/R}$, and L_{RL} is only in the range of 0.01 μH to .2 μH [27], [31]. In addition, series resistance, R_{RL}, is so small as to be negligible; R_{IL} and $R_{I/R}$ are at most several hundred ohms for hand/metal ESD, which

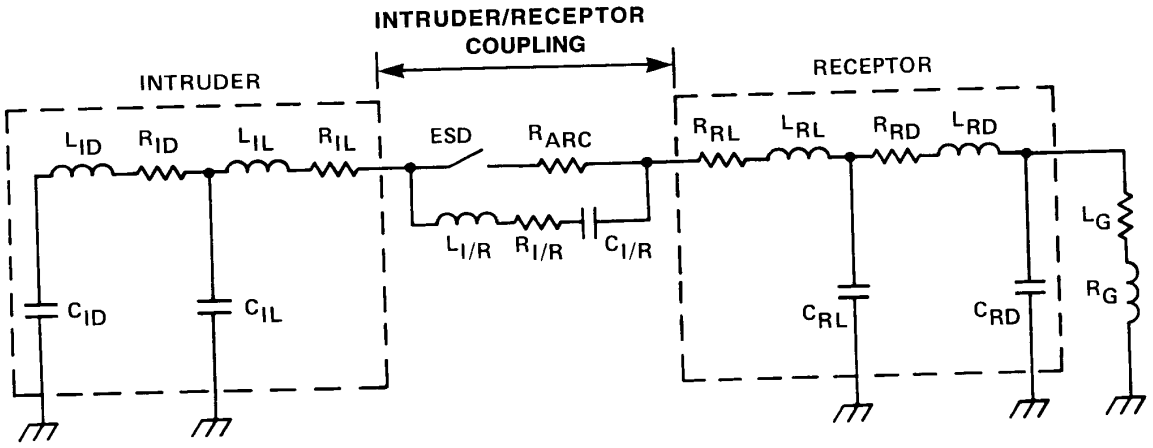

Fig 17
Capacitance/Inductance Model for Participants in an ESD Event

includes hand-to-metal impedance. Thus, even though these capacitors are small, the extremely low inductance and low resistance in the discharge paths for C_{IL}, $C_{I/R}$, and C_{RL} may allow a discharge current spike of relatively high amplitude (see [9] for additional information). This current spike routinely reaches tens of amperes for charge voltages of only a few kilovolts, and under some conditions for furniture ESD can exceed 100 A. The initial spike duration is usually less than a few nanoseconds.

The subnanosecond rise time and relatively high peak amplitude of the initial spike result in initial slopes for discharge current that may exceed 10 A/ns/kV or 15 A/ns/kV of initial charge voltage on C_{IL}.

The capacitances associated with intruder and receptor areas more distant from the ESD, C_{ID} and C_{RD} respectively, have appreciably larger inductances; each has a value lying from 0.1 μH to over 2 μH [27], [31]. While resistance R_{RD} is normally negligible for a metallic equipment chassis, R_{ID} is tens or hundreds of ohms for a human intruder. As a result primarily of their large associated series inductances, the distant capacitances do not play a major role in generating the fast initial slope.

Instead, they cause the main discharge current wave that follows the initial slope. It has a slower rise time and longer duration.

The shape of the main discharge current wave is also affected by any equipment-ground connection that may exist. This connection is represented by L_G and R_G in Fig 17. Normally R_G will be very small, but L_G will normally be about 1 μH per meter of ground wire. The ground path represented by R_G and L_G will act to shunt a portion of the main discharge current around C_{RL} and C_{RD}.

The risetime of the main discharge current wave is typically 2–30 ns or more, and its duration is typically 30 ns to over 100 ns. It is undirectional for body/finger and hand/metal ESD, and usually oscillatory for furniture ESD. Its amplitude ranges from less than 1 A for body/-finger discharge, to a few amperes or tens of amperes for body/metal or hand/metal ESD, to hundreds of amperes for furniture discharge. For both body/ finger and hand/metal ESD, the peak amplitude of the main discharge current wave is typically less than half of the initial spike amplitude. For furniture ESD, its amplitude is typically greater than that of the initial slope; as a result, the initial fast-rising slope often appears simply as a fast leading edge for a fraction of the main discharge peak amplitude; no, or very little, initial spike is apparent.

The circuit of Fig 17 is only a rough approximation to the actual situation, which is better characterized by a model with distributed parameters than by a lumped parameter model

[30]. Nevertheless, lumped parameter models constitute a practical basis for computer simulations of ESD currents. Such simulations agree reasonably well with measured waveforms [27], [31].

6.5.3 Electrical Parameters of Human Bodies. Table 3 gives calculated values of capacitance to free space, as well as calculated values for series inductance, based on spherical or cylindrical approximations of the human body segments involved in an ESD [11], [31].

While the geometry of various body segments is largely responsible for determining their effective inductances and capacitances, their resistances depend on many highly variable, nongeometric factors. Bulk resistance of various body segments have been estimated [11], [12]. However, in both a body/finger and a hand/metal ESD, skin resistance is in series with bulk resistance, and effective skin resistance is believed to vary not only with humidity, but also with the chemistry of individual skin secretions. In a hand/metal discharge, additional factors not relevant to a body/finger discharge include area of contact with the metal object and the force between the object and the skin. For example, a bracelet may be in fairly loose skin contact over a substantial area, while a tool or a key may be held with different amounts of force over areas of widely differing sizes (see Fig 3).

Since the effective resistance depends on so many variable factors, appropriate resistance values for modeling purposes may best be determined by comparing computer models incorporating the more readily calculable L and C values of the body with a number of actual ESD events. Results of such comparisons give ranges of 300–1000 Ω for the total resistance in a hand/metal ESD event [27].

Table 3
Approximate Dimensions, Estimated Capacitance, and Estimated Inductance for Various Sections of the Human Body [31]

	Diameter (cm)	Length (cm)	C (pF)	L (μH)
Fingers holding key	2	6	2	.02
Entire hand holding key (to wrist)	7.5	12.5	5	.02
Forearm (wrist to elbow)	9	30	10	.1
Full arm (wrist to shoulder)	9	60	20	.27
Torso (shoulder to waist)	30	60	20	.13
Whole body (torso plus lower body)	30	120	60*	.43

*The calculated capacitance values are those that would exist for a human who is not in close proximity to a ground plane. For a person standing on a ground plane, the proximity of the ground plane to the feet would result in a much larger whole-body capacitance. For a person who is standing on a ground plane, the whole-body capacitance can be 100 pF to 150 pF.

6.5.4 The Two-Resistor-Inductor-Capacitor (RLC) Circuit Model for Human ESD. A two-RLC circuit model has become generally accepted to approximate the electrostatic discharge from a human body, including the fast initial pulse from the hand [31]. The circuit model is shown in Fig 18 and includes two parallel RLC paths, one representing the hand and the other the body. The receptor is modeled as an ideal ground.

Values for the hand capacitance to free space as well as for hand resistance and for hand inductance, corresponding with local parameters C_{IL}, R_{IL}, and L_{IL}, in series with R_{RL}, L_{RL},

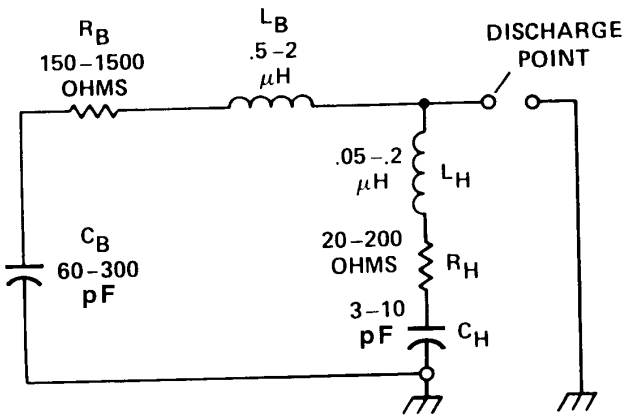

Fig 18
The Two-RLC Model for Human ESD in Region I

and C_{RL} in Fig 17, are shown as C_H, R_H, and L_H respectively. Also, C_H, R_H, and L_H include the effect of $C_{I/R}$, $R_{I/R}$, and $L_{I/R}$, which are in parallel with the previous series components.

Parameters for the body are C_B, R_B, and L_B. The parameter C_B corresponds to the series combination of C_{ID} and C_{RD} of Fig 17; however, R_B corresponds to the total of R_{IL}, R_{ID}, R_{RL}, and R_{RD}; L_B corresponds to the total of L_{ID}, L_{IL}, L_{RD}, and L_{RL}. As a result, the initial current pulse is provided by C_H, R_H, and L_H, and the main discharge current wave is provided by C_B, R_B, and L_B.

Therefore, Fig 18 emphasizes independent generation of the initial spike via the hand/forearm RLC, and the main discharge wave via a body RLC. The parameter values shown in Fig 19 are typical of the ranges for hand/metal ESD.

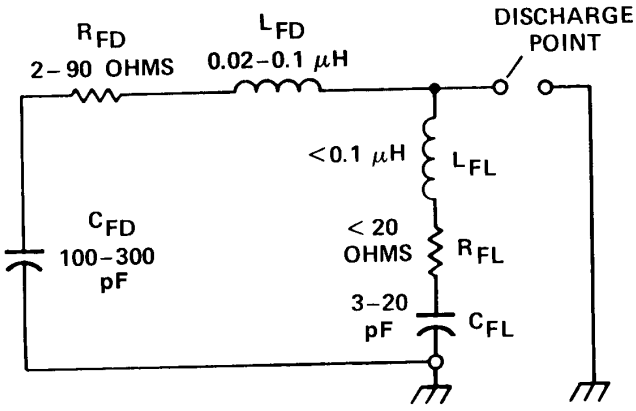

Fig 19
The Two-RLC Model for Furniture ESD

6.5.5 The Two-RLC Model for Furniture ESD. In addition to human ESD, furniture ESD can also be explained and modeled by a two-RLC circuit, as shown in Fig 19.

Based on both measurements and calculations, intruder parameters for furniture such as carts, with and without associated human bodies, include capacitance C_{FD} on the order of 100–300 pF, resistance R_{FD} from a few ohms to several tens of ohms, and inductance L_{FD} in the range of a few tens of nanohenries [12], [23]. These distant furniture parameters correspond with C_B, R_B, and L_B in Fig 18 for human ESD. The equivalent of hand parameters C_H, R_H, and L_H in the same figure also exist for furniture; the small local area of the object within a few centimeters of the discharge usually has a low inductance to the point at which the ESD takes place. This low inductance will cause a fast initial slope or even an initial spike.

It is possible that C_{FL} is equal to or exceeds C_H, while R_{FL} and L_{FL} may be presumed to be very much smaller than R_H and L_H respectively. However, these parameters have not been reported on to date.

As mentioned in 6.5, when the furniture is large, such as a chair or cart, the initial spike can be swamped by the main discharge wave; it may appear as a 30-50% subnanosecond initial slope and will lose its initial spike character as such.

If a person is in electrical contact with a mobile furnishing that contains sharp edges, the voltage on the furnishing and the person may be less than the highest value that can be sustained by the person alone. However, the total capacitance will be higher than that of either the person or the object [32].

The relationship between a person pushing a rolling metal cart and a receptor in the form of an equipment console has been modeled [12]. Results indicate that the maximum calculated peak current obtained from the cart pushed by a person charged to 10 kV was 770 A, with a rise time of 2–3 ns. From [12], the component values for the circuit model of Fig 19 for distant capacitance C_{FD}, inductance L_{FD}, and resistance R_{FD} are 229 pF, 0.03 μH, and 2 Ω respectively. The total value of each of these circuit components includes both the furniture and the charged human body. Reference [23] shows peak currents of a few tens of amperes to over 100 A. Specifically, 170 A was measured for a charge voltage of 10 kV. The model in [12] did not include local parameters C_{FL}, L_{FL}, or R_{FL}, but the fast rise times of [23] indicate that they exist.

6.5.6 Adjustment of ESD Event Models for Receptors of Different Sizes. Receptor component values used in circuit models like that of Fig 17 may change significantly. Even though the equivalent circuit configuration of the intruder may remain the same, changes in the receptor will result in waveform changes. The interrelationships among all of the capacitances, including those of the receptor, must be taken into account. Therefore, in order to develop electrical models of ESD events, it is necessary to include standardized characteristics for the receptor.

A measurement target [3] mounted in a large plane receptor has been used for virtually all work to date on characterizing discharge currents in both human and furniture ESD, and for all models of ESD. A typical size is 1.5 x 1.5 m [1], but the solid wall of a shielded enclosure is also commonly used to measure waveforms [15].

Therefore, all of the ESD circuit models of 6.5.1 through 6.5.5 were based on using a very large ground plane as the receptor. In other words, C_{RL} in Fig 17, the local receptor capacitance to ground or the nearby surroundings, is quite large, ranging from 200 pF to over 500 pF.

As a first approximation, receptors may be categorized as large or cabinet-size units, medium size units representing desk-top equipment, and small size units such as calculators or telephones.

As a practical matter, the capacitance of large cabinet-sized receptors is close enough to that of the large ground planes that have been used to collect ESD waveform data. As long as the receptor capacitance is several times the largest intruder capacitance, no further increase in receptor capacitance is significant because intruder and receptor capacitances are effectively in series.

However, the waveforms that result for medium-size receptors may be different, and for small receptors significant waveform changes may result [17].

Since both of the two-RLC models assume the receptor is an ideal ground, changes in the RLC parameters are required in order to model different receptors. If C_{RL} in Fig 17 is comparatively large, for example, as it is for the large planar receptor, then C_B and C_H in Fig 18 will be essentially equal to C_{ID} and C_{IL} of Fig 17, respectively. On the other hand, for a small receptor, the capacitance of the receptor is comparable with C_{IL} and probably less than C_{ID}. If the small receptor is 60 cm to 80 cm from ground, its capacitance will be on the same order as that of a sphere of 12–15 cm diameter, or 7–10 pF [30]. This is comparable with CIL for a hand or hand/forearm [30], so that the equivalent series capacitance, which is what is expressed by C_H in Fig 18, will be approximately halved. This will diminish both the amplitude and the duration of the initial current pulse.

C_B in Fig 18 is affected even more by receptor size. It represents the series combination of intruding body capacitance C_{ID} in Fig 17 with receptor distant capacitance C_{RD} in the same figure. For small ungrounded receptors, C_{RD} in effect does not exist, so that the distant intruder capacitance, C_{ID}, is in series with the 7–10 pF capacitor C_{RL} to make up C_B in the two- RLC circuit of Fig 19. The implication of this extremely low effective body capacitance is that there will be a negligible main discharge wave with a small ungrounded receptor that is 60–80 cm from ground.

For small grounded receptors, the ground wire path, including its stray capacitance, acts as C_{RD}. Therefore, the main discharge wave will still exist, although at a reduced level compared with the main discharge wave that would exist for a large receptor.

6.5.7 Multiple Discharge Models. Although multiple discharge phenomena are described in 6.4.4, no model for the phenomenon of multiple discharge is generally accepted.

7. Representative Measurements of Specific Electromagnetic Interface (EMI) Effects Generated by or Related to ESD

This section describes the general EMI parameters, due to ESD, that are believed to cause malfunction of electronic equipment. Representative waveforms and parameter ranges are included.

7.1 Injected Current. As far back as 1968, data have been published on the ESD current waveform [36]. More recent data using both 400 MHz and 1 GHz instrumentation have shown the existence of the fast initial slope and, in the case of most hand/metal ESD events and some furniture ESD events, the initial spike [13], [14], [15], [19], [20], [21], [22], [23], [24], [26], [27], [28], [29], [30], [31], [35], [37]. The most recent published work is usually relied on in this section, since it usually, if not always, involves the most up-to-date measuring techniques and equipment.

Fig 20 shows a representative fast-rise human ESD current wave, as measured with 400 MHz instrumentation: i.e., current transducer, cabling, and oscilloscope [26]. It resulted from a hand/metal discharge with the intruder initially charged to 4 kV. In this specific case, the discharge electrode of the intruder was a ring on a finger, and the approach speed was fast. The wave that resulted had an initial current pulse and an extremely fast rise time, as is typical of region I waveforms for human ESD. Peak current is 19.2 A, and the displayed rise time is limited to just under 1 ns by the 400 MHz oscilloscope used for this particular test. Initial slope, approximated as the ratio of the peak current to the time required to reach peak, is thus greater than 20 A/ns; how much greater is not known, in view of instrumentation bandwidth limitations.

Fig 21 shows a typical region I hand/metal discharge current, also at 4 kV, using 1 GHz instrumentation (current transducer, connectors, cables, and oscilloscope) [37]. Fig 22 shows discharge current resulting from a similar ESD on a time scale of 200 ps per division, instead of 10 ns per division [37].

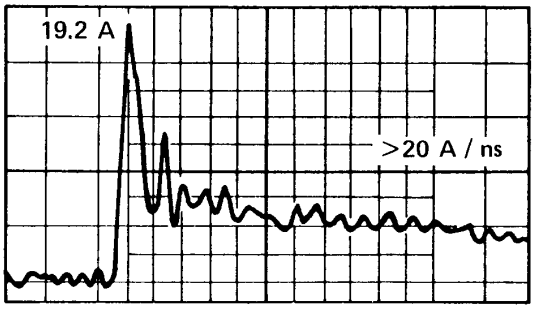

Fig 20
Typical Fast-Rise ESD Current Wave From Hand With Ring, Showing Initial Current Pulse and Main Discharge Wave [26]

NOTES: (1) 400 MHz oscilloscope and current-viewing resistor.
(2) 4 kV initial charge voltage (region I); body/metal discharge, fast approach; 4 ns/division, 4 A/division.

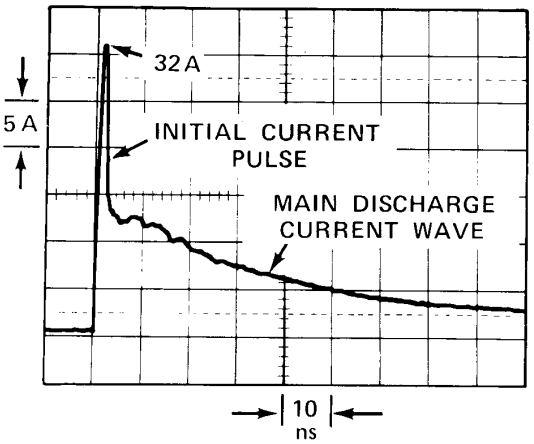

Fig 21
Measured Discharge Current From a Hand/Metal ESD [37]

NOTES: (1) 1 GHz oscilloscope and current-viewing resistor.
(2) 4 kV initial charge voltage (region I); body/metal discharge, fast approach; 10 ns/division, 5 A/division.

The wave of Fig 21 includes the steep yet narrow initial current pulse, as well as the main discharge wave. Fig 22 shows just the initial spike. The peak current in Fig 21 is about 32 A, and since the test was performed at an initial charge voltage of 4 kV, normalized peak current is 32/4 = 8 A/kV, while for Fig 22 it is about 8.5 A/kV. The risetime from Fig 22 is about 350 ps, approximately equal to the risetime of the oscilloscope/current transducer combination used for the test. Thus, the actual risetime of the ESD current only known to be faster than the 350 ps figure; it is probably less than 150–200 ps, or else the measured 350 ps risetime would be 400 ps or higher. More important is the rising slope of the wave. In Fig 22 it is about 100 A/ns. Normalized rising slope is thus 100/4 = 25 A/ns/kV.

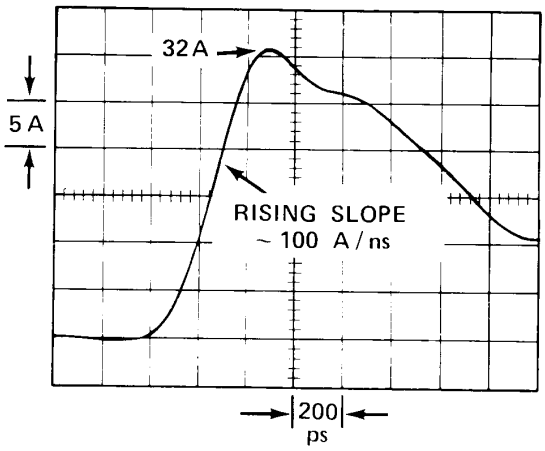

Fig 22
Same as Fig 21 Except 200 ps/Division

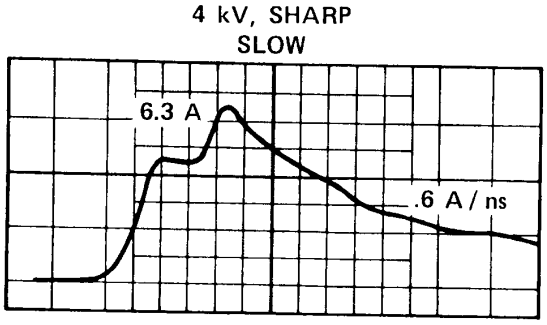

Fig 23
Typical Slow-Rise ESD Current Wave From Hand With Sharp Metal Object, Showing No Initial Current Pulse [26]

NOTE: 4 kV initial charge voltage (region I); body/metal discharge, slow approach; 10 ns/division, 2 A/division.

In contrast with the fast-rise human ESD examples shown in Figs 20 through 22, Fig 23 is a typical slow-rise human ESD current wave with no initial current pulse. This current wave resulted from a body/metal discharge with the intruder again initially charged to 4 kV, but the discharge electrode was a sharp pointed electrode and the approach speed was slow. Thus, the ESD took place in region II. Note that this is an example of the fact that even though the voltages for Figs 20 through 23 were the same, i.e., 4 kV voltage regions dominated in these examples by electrode shapes, they varied between regions I and II.

The front in Fig 23 displays the notch that is typical of some region II and most region III waveforms for human ESD [20], [21], [26]. The difficulty of defining a meaningful rise time for this kind of wave has contributed to the attempt to use initial slope to describe ESD current wavefronts.

Measuring the fastest rising slope from Fig 23 and assuming it would last from 10 to 90% of wave peak yields a "fastest rise time" of 2–3 ns; simply measuring the 10% to 90% time difference in Fig 23 gives 8 ns. This is an important point; a simple 10% to 90% rise time figure (e.g., 8 ns) would be a misleading description for a front that rises from 10% to 50% in less than 2 ns. Use of rise time to characterize complex wavefronts is therefore deprecated. In any case, all parts of the front of Fig 23 are slow compared to the front of the initial current pulse of Figs 20 through 22.

Many variations of these two broad waveform categories exist, and they are covered in greater detail in various references [13], [14], [22], [25], [28], [35], [36].

7.1.1 Initial Current Pulse. Reasonable worst-case values for the most important parameters of the initial current pulse for hand/ESD have been developed on the basis of data reported by a number of investigators [14], [15], [22], [23], [24], [26], [29]. These parameters are peak current, risetime or initial slope, and duration. Ranges for these are given for fast approach speed in Table 4; peak current and initial slope are normalized for charge voltage. (Comparable information for the initial slope on initial pulse for furniture ESD is not available in sufficient quantity and detail in the literature at the present time.)

Table 4
Reasonable Worst-Case Values for Initial-Current Pulse Parameters for Hand/Metal ESD in Fast Approach (400 MHz and 1 GHz Oscilloscopes)

Parameter	Value When Using 400 MHz Oscilloscope	Value When Using 1 GHZ Oscilloscope
Normalized peak current	3–6 A/kV	5–10 A/kV
Rise time	.7–.9 ns	.25–.35 ns
Normalized rising slope	3–6 A/ns/kV	5–25 A/ns/kV
Duration	2–4 ns	1–3 ns

Values in Table 4 are included for two oscilloscope bandwidths, 400MHz and 1 GHz, to illustrate the importance of instrumentation bandwidth on the results. It is anticipated that when ESD is viewed with still higher bandwidth-current-viewing resistors and oscilloscopes, the ESD event will be shown to be faster.

Depending on charge voltage and approach speed, the initial spike can become much smaller, in which event it will start to blend into the start of the main discharge wave until it finally disappears altogether. In this case, the main discharge wave will constitute the entire ESD current. The consequence of this situation is dominance by the main discharge wave characteristics: relatively long rise time, relatively low initial slope, and relatively low peak current.

7.1.2 Main Discharge Current Wave. The main discharge current wave is essentially independent of the size of the initial current pulse for hand/metal ESD or of the duration of the initial slope for furniture ESD. Reasonable worst-case figures for main discharge wave parameters of hand/metal ESD are given in Table 5, and parameters for furniture ESD are given in Table 6. There is no need to provide performance for different oscilloscope bandwidths, since the phenomena being measured are no faster than the rise time of the specified 400 MHz instrumentation.

Table 5
Reasonable Worst-Case Values for Main Discharge Current Wave Parameters for Hand/Metal ESD (≥ 400 MHz Oscilloscope)

Parameter	Value
Normalized peak current	3 A/kV
Rise time	2 ns to 20 ns
Duration	30 ns to 80 ns

Table 6
Reasonable Worst-Case Values for Main Discharge Current Wave Parameters for Furniture ESD

Parameter	Value
Normalized peak current	7 A/kV to 25 A/kV
Rise time	< 10 ns
Duration to axis crossing	12 ns to 35 ns

7.1.3 Multiple Discharges. As indicated in section 6.4.4, when multiple discharges occur, successive discharges are initiated at lower charge voltages than the first discharges. As a result, the subsequent discharges can have much faster initial slopes than the first discharges, i.e., they may display characteristics of the lower end of region II or even of region I, instead of region III or the upper end of region II, in which the earliest ESDs presumably originate.

Fig 24 shows the results of a single hand/metal ESD from a high charge voltage, i.e., one taking place at 15 kV, or in region III [37]. The 1 GHz oscilloscope that was used to obtain the data was set up to retrigger immediately after each wave, so that all the waves in a single multiple ESD could be shown on the same display.

Note that all five of the waveforms in Fig 24 occurred during what is normally thought of as only one hand/metal ESD, i.e., only a single approach to the receptor. The voltage regions in which each of the five discharges apparently took place are marked on the figure. It is striking that the highest peak was the second one to occur. The first to occur, marked as taking place in region III, had a much lower peak; it is presumed that corona effects reduced its amplitude. The second peak occurred at a lower charge voltage, where there presumably was lower corona, and actually had a higher peak. It is assumed that it probably took place in region II. The three subsequent, final waves took place in region I, i.e., rise times were in the nanosecond or subnanosecond range, and the waves displayed initial spikes as might be expected.

Fig 25 shows another hand/metal multiple ESD with all of the same conditions as for Fig 24 [37]. Two notched waves occurred first, presumably in region III. Following them was a wave with an extremely large initial spike; it and all subsequent waves were most likely in voltage region I.

Generation of subsequent multiples, with fast initial spikes, can be the reason why discharges from higher voltages can cause upsets otherwise caused only at quite low voltages.

7.2 Electromagnetic Fields. The electric and magnetic fields produced by an electrostatic discharge will vary depending upon the charge voltage and other parameters, but it is possible to identify general characteristics.

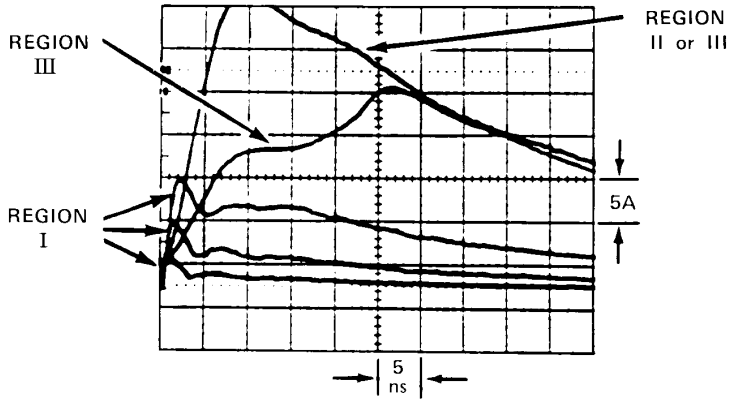

Fig 24
Multiple (Five) Human ESDs From the Same ESD Event [37]

NOTE: 15 kV, 5 A/div, 5 ns/div; 1 GHz scope.

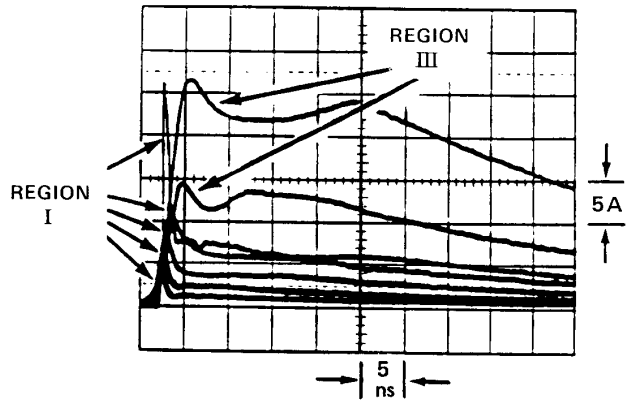

Fig 25
Multiple (Seven) Human ESDs From the Same ESD Event [37]

NOTE: 15 kV, 5 A/div, 5 ns/div; 1 GHz scope.

Spectra are broadband, i.e., from low kilohertz to low gigahertz. The fields are transient. Their maximum levels are on the order of a kilovolts/meter for the electric field and a few tens of amperes/meter for the magnetic field at a distance of 10 cm from the discharge [38].

Field levels and characteristics produced in any ESD are dependent on the discharge current waveform, as well as on the intruder and receptor.

The intruder and receptor, as a set, act as an antenna; the radiated energy levels will vary as their geometry, shapes, and materials are changed.

Data have recently been reported on both theoretical and experimental work on fields generated by ESD [38]. All of the discharges were generated by a commercial ESD simulator. Measurements were made of the electric field at a distance of 1.5 m from the discharges, and of the receptors to which the discharges occurred. Newly designed, broadband, time-domain antennas of several types were used for these measurements by the US National Institute of

Standards and Technology (NIST). [This was formerly known as the National Bureau of Standards (NBS).] These antennas have bandwidths from 40 MHz to several gigahertz.

H-field (magnetic field) calculations were made based on measured discharge currents. Predictions were also made for both E and H fields at distances closer than 1.5 m, based on a generally acceptable correlation between measured and calculated results for the E fields (electric fields) at 1.5 m.

The data were taken using an ESD simulator in a fixed location, discharging to one of several different receptors. Tests were performed from voltages of 1 kV to as high as 12 kV. Only at the lower voltages, i.e., primarily in region I, do the subnanosecond rise times for discharge current have counterparts in subnanosecond measured E-field rise times. In addition, discharges from 2–4 kV, again in region I, excited fields with the largest peak magnitudes. The low-voltage, fast rise time (i.e., region I) discharges might therefore cause the most severe upset to many equipment victims.

Theory showed that near E fields and near H fields depend directly on the ESD current, and that far E fields and far H fields depend on the time derivative of the current.

Measured E-field magnitudes in some cases exceeded 100 V/m at a distance of 1.5 m from the discharge point. Calculated H-field magnitude reached.3 A/m at the same distance, specifically for a 4 kV charge voltage.

Calculated values for both E and H fields reached over 4000 V/m and 15 A/m respectively at a 10 cm distance from the discharge.

Figs 26 through 35 show the measured results from reference [38]. For all of the data in [38], the so-called "clean time," or time before the first reflection from the walls and ceiling of the room was 10 ns. Thus, most of the data should be quite valid as the features of interest generally required less than this time to occur. However, with the plate and trash can experiments of Figs 33, 34, and 35 this is not the case; data beyond the 10 ns point in time in these three figures therefore must contain significant reflection components from the walls and ceiling. The authors of [38] point out that this may represent a realistic situation for actual ESD threats to equipment, however, as such threats will typically occur in rooms of finite dimensions.

Figs 26 through 29 give measured E-field results from reference [38] for 1 kV, 2 kV, 4 kV, and 6 kV charge voltage tests, respectively.[8] In all four cases, discharges were made directly to a ground plane, and the antenna was located 1.5 m from the discharge. Fig 30 shows the calculated H field, also 1.5 m from the discharge, for the 4 kV charge voltage.

Figs 31 and 32, again from [38], give calculated E-field and H-field magnitudes, respectively, for various distances from the discharge, ranging from 1.5 m down to 10 cm; both sets of calculations were performed for a 4 kV charge voltage.

Finally, Figs 33, 34, and 35 give the measured E field radiated respectively by a vertical .9 m x .9 m metal plate excited by a 5 kV discharge, by a metal chair excited by a 3 kV discharge, and by a metal trash can excited by a 6kV discharge. All three tests were done over a ground plane, and the discharge itself was purposely obscured from the antenna by the object to which the discharge was made.

The spectral content of fields from ESD is recognized as containing significant energy to at least 2 GHz [18], [19], [38], and perhaps as high as 5 GHz [38].

8. Conclusion

As this guide indicates, the characteristics of a specific ESD event will vary significantly as a function of the exact conditions associated with the event. However, this guide also indicates

[8]Note that for Figs 26 through 35, the position of the start of the wave versus $t = 0$ is arbitrary. Some of the waves result from a deconvolution process that effectively removes the known frequency limitations of the antenna. The position of zero time was not preserved as the data was operated on during that process. For other waves, the oscilloscope trigger versus the start of the ESD was uncertain. The validity of the data is believed to be unaffected by this uncertainty.

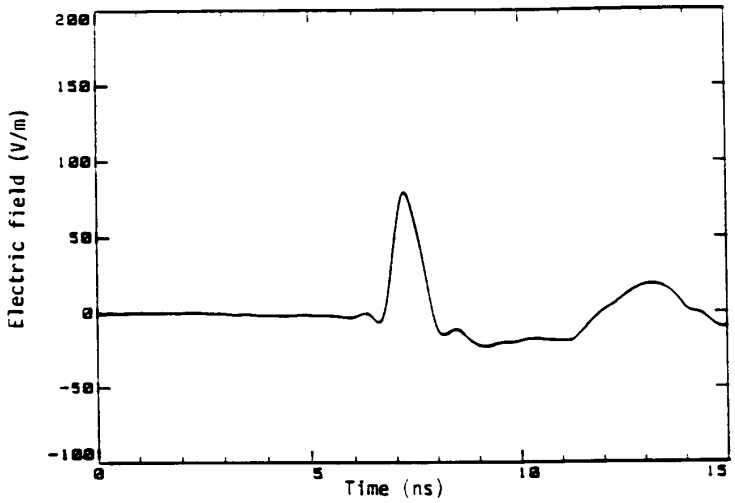

Fig 26
Measured Vertical Electric Field for a 1 kV ESD Simulator Discharge to a Ground Plane [38]

NOTE: Antenna 1.5 m from the discharge.

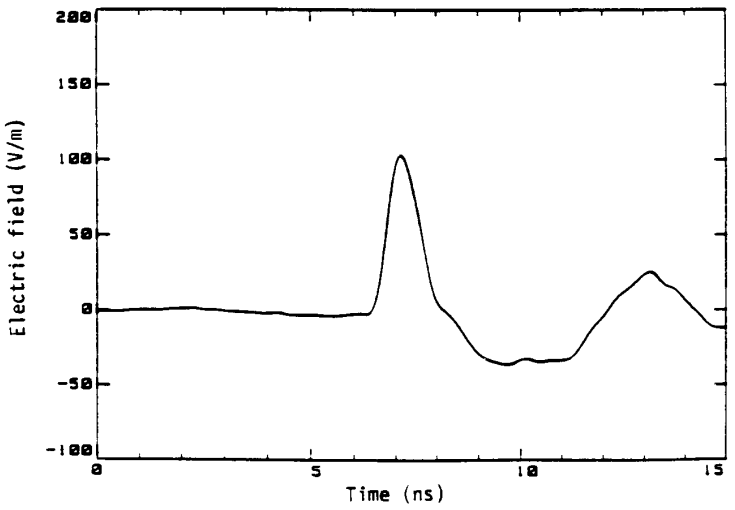

Fig 27
Measured Vertical Electric Field for a 2 kV ESD Simulator Discharge to a Ground Plane [38]

NOTE: Antenna 1.5 m from the discharge.

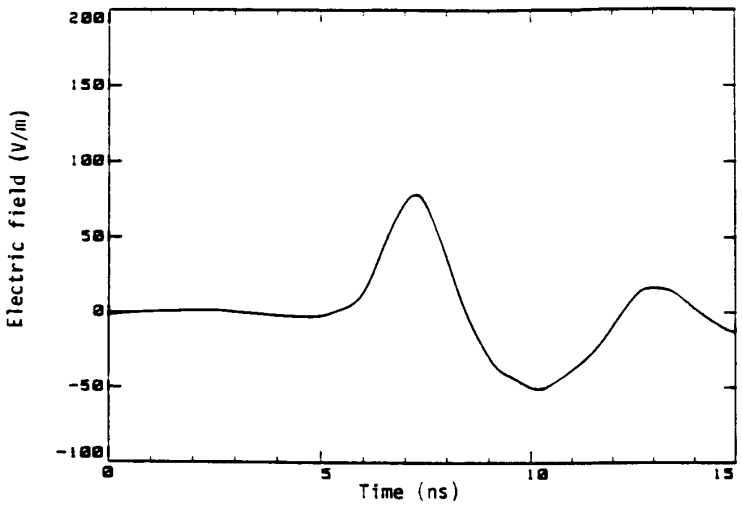

Fig 28
Measured Vertical Electric Field for a 4 kV ESD Simulator Discharge to a Ground Plane [38]

NOTE: Antenna 1.5 m from the discharge.

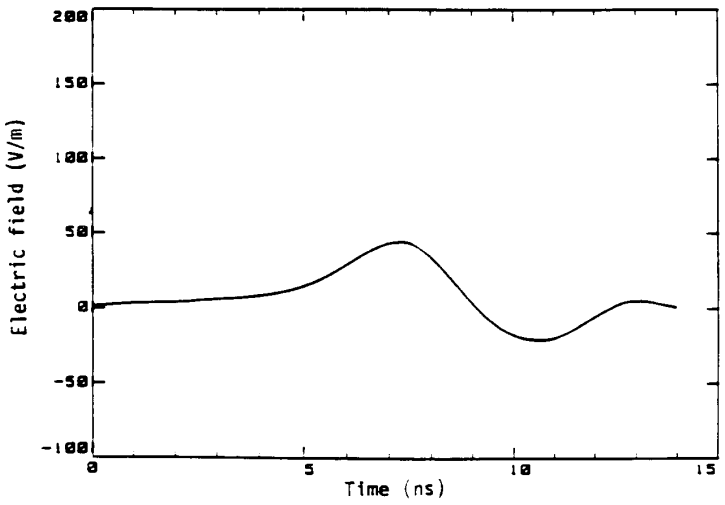

Fig 29
Measured Vertical Electric Field for a 6 kV ESD Simulator Discharge to a Ground Plane [38]

NOTE: Antenna 1.5 m from the discharge.

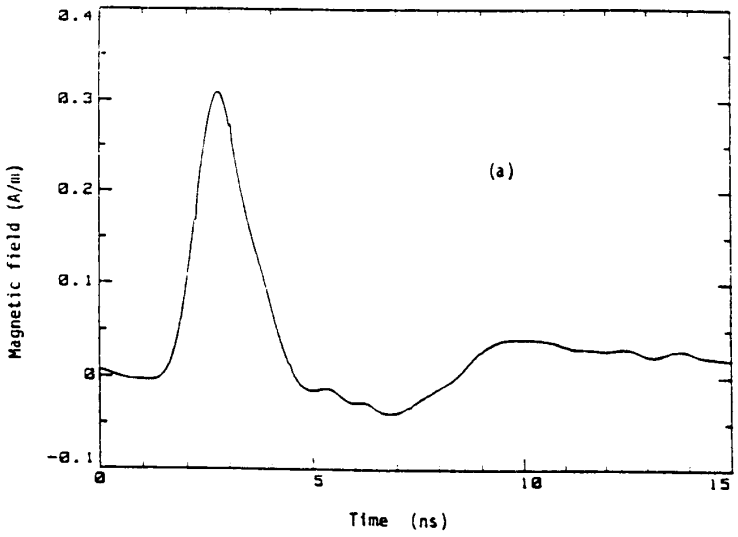

Fig 30
Calculated Magnetic Field for a Discharge to a Ball Target at 4 kV [38]

NOTE: Antenna 1.5 m from the discharge.

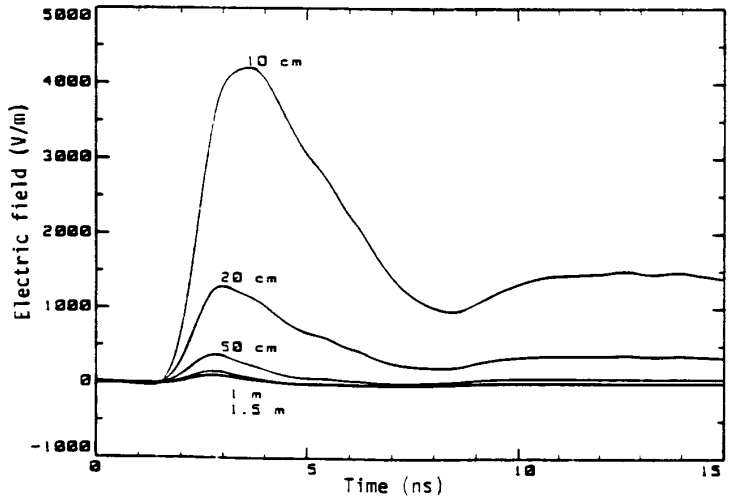

Fig 31
Calculated Vertical Electric Field for a Discharge to a Ball Target at 4 kV [38]

NOTE: Antenna at various distances from the discharge.

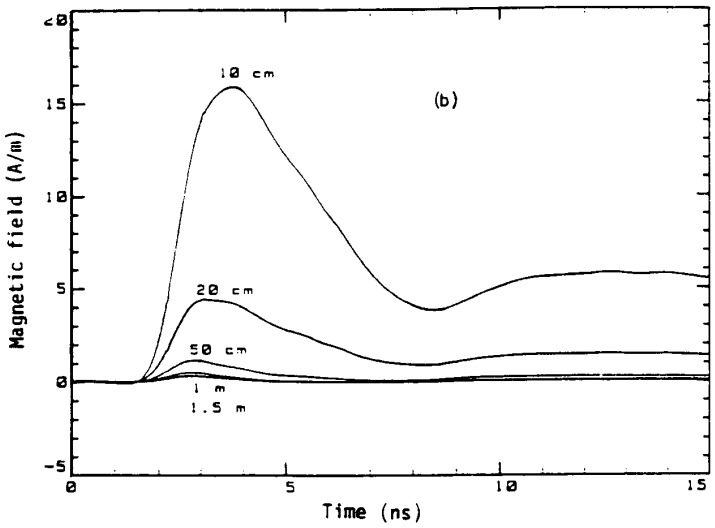

Fig 32
Calculated Magnetic Field for a Discharge to a Ball Target at 4 kV [38]

NOTE: Antenna at various distances from the discharge.

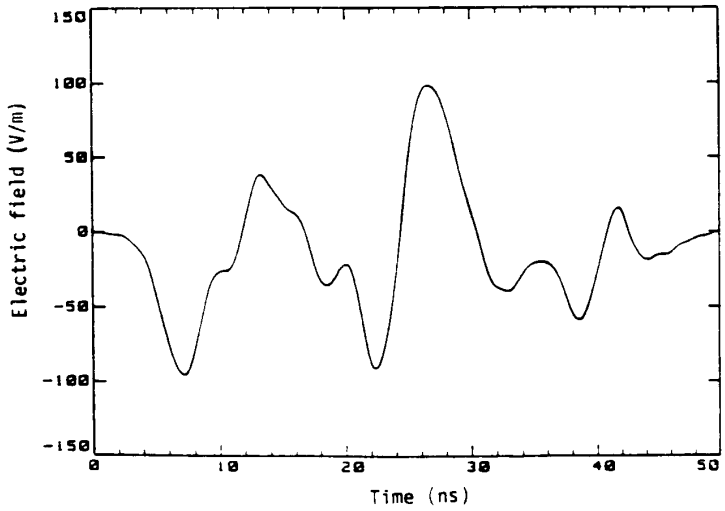

Fig 33
Measured Vertical Electric Field Radiated by a Vertical Square Metal Plate Over a Ground Plane; 5 kV Spark [38]

NOTES: (1) Antenna 1.5 m from plate; ESD simulator; discharge behind plate.
(2) Antenna clean time approximately 10 ns.

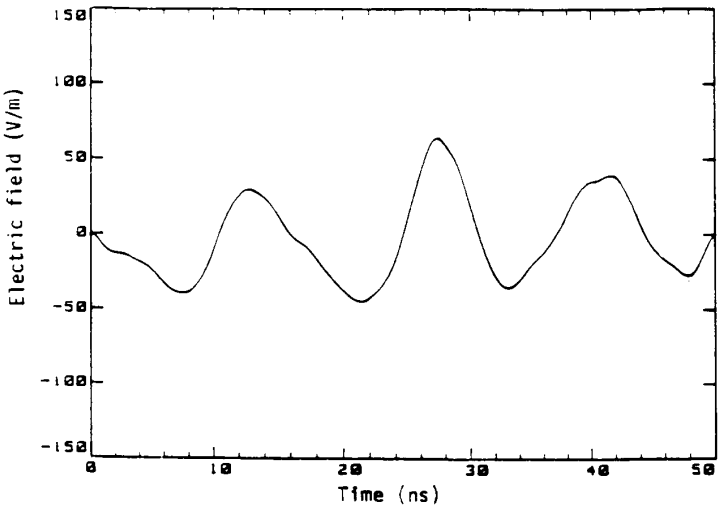

Fig 34
Measured Vertical Electric Field Radiated by a Metal Chair Over a Ground Plane; 3 kV Spark [38]

NOTES: (1) Antenna 1.5 m from discharge; ESD simulator; discharge behind chair.
(2) Antenna clean time approximately 10 ns.

that there are limits to this variation. It is therefore possible to identify the characteristics of reasonable worst-case ESD events. While a knowledge of these reasonable worst-case events can be useful in the development and interpretation of ESD test standards, they are not themselves intended for direct use as test standards.

The conclusions of this guide are that the two ESD current waveforms shown in Figs 36 and 37 represent reasonable worst-case human ESD current waveforms, and that the two ESD current waveforms shown in Figs 38 and 39 represent reasonable worst-case furniture ESD waveforms. The waves of Figs 36 and 38 take place in voltage region I; those of Figs 37 and 39 take place in region II or III. All four waveforms are based on measurements made using 1 GHz instrumentation. 8.1 and 8.2 give information on the influence of charge voltage and receptor size, respectively. Table 7 summarizes the relationship of charge voltage and receptor size to worst-case ESD current waveforms by indicating the waveform that corresponds with each condition in the matrix.

8.1 Influence of Charge Voltage Control. If the environment is such that charge voltages are controlled to known levels, then the peak ESD current for each worst-case waveform may be estimated by using the known maximum charge voltage in the controlled environment (Figs 36 through 39). If charge voltage is not specifically controlled, then the worst-case peak ESD current should be assumed to be the maximum value associated with each of the four figures.

In addition, the range of charge voltages in the environment will determine whether region II or III waveforms of Figs 37 and 39 apply or if only the lower charge voltage, region I of Figs 36 and 38, applies.

8.2 Influence of Receptor Size. For direct ESD, the receptor itself will be important in determining the worst-case ESD event. As indicated in 6.5.6, the amplitude and duration of

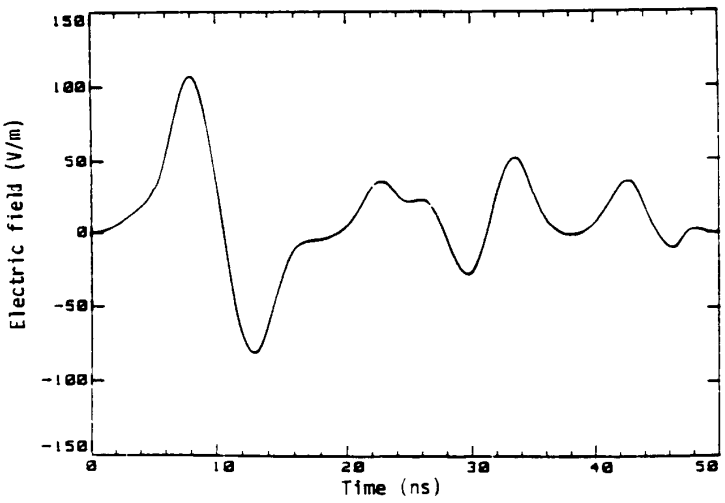

Fig 35
Measured Vertical Electric Field Radiated by a Metal Trash Can Over a Ground Plane; 4 kV Spark [38]

NOTES: (1) Antenna 1.5 m from discharge; ESD simulator; discharge behind can.
(2) Antenna clean time approximately 10 ns.

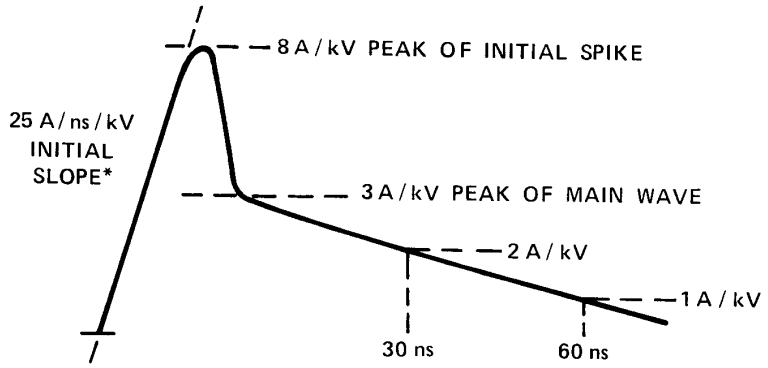

Fig 36
Region I Hand/Metal ESD

NOTE: 4 kV maximum charge voltage.

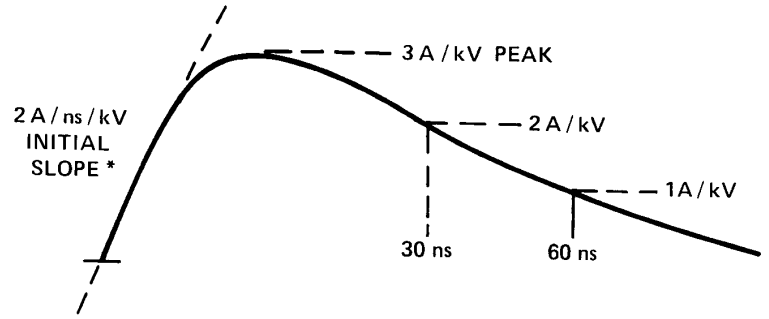

Fig 37
Region II or III Hand/Metal ESD

NOTES: (1)15 kV maximum charge voltage (very little data for human ESD exists above 15 kV).
(2) At voltages above 8 kv, multiple discharges may occur; therefore, the waveforms of both Figs 36 and 37 may well exist in a single ESD event.

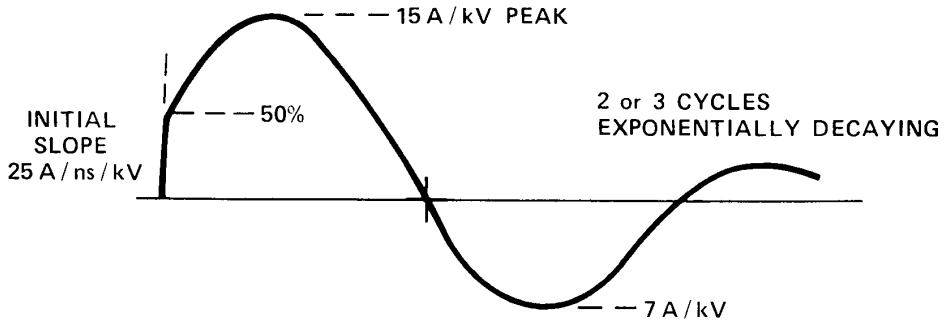

Fig 38
Region I Furniture ESD

NOTE: 4 kV maximum charge voltage.

the ESD current waveform is partially dependent on the size of the receptor. The worst- case waveforms shown in Figs 36 through 39 apply for relatively large receptors, with surface areas exceeding 1 m^2. For smaller receptors, peak amplitudes and durations will be less than those of Figs 36 through 39. In addition, the characteristics of worst- case direct ESD events are related to equipment location as well as to equipment size. For example, desktop equipment is normally inaccessible to direct furniture ESD.

For indirect ESD, worst-case waveforms and their associated fields are unrelated to the size of the equipment victim, since it is not directly involved in the event; instead, they depend on the sizes of the intruder and receptor. Indirect ESDs will often involve large receptors such as desks, and the ESD currents will therefore look like those of Figs 36 through 39 without modification. The ESD-related fields at the equipment victim will, of course, depend on its location with respect to the intruder, to the receptor, and to the discharge itself.

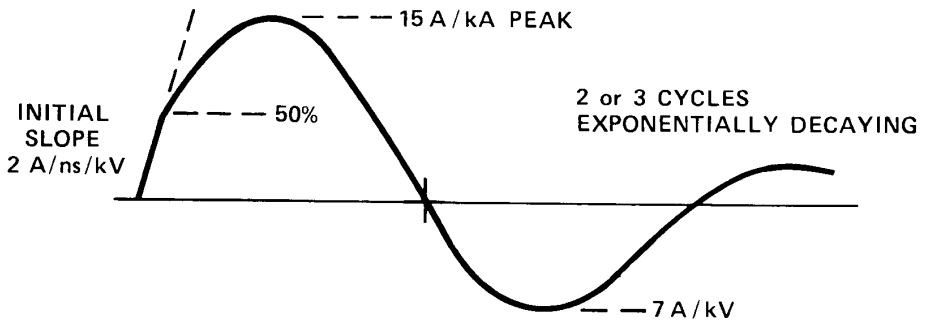

Fig 39
Region II or III Furniture ESD

NOTE: 8 kV[1] maximum charge voltage.

[1]Because furniture typically has sharper radii, corona will prevent the development of extremely high voltages.

Table 7
Reasonable Worst-Case ESD Waveforms for Different Equipment and Environments*

Charge Voltage Control Level	Equipment Size	Type of ESD Threat			
		Hand/Metal		Furniture	
		Direct	Indirect	Direct	Indirect
To < 4 kV	Large (e.g, floor standing cabinet)	36	36	28	38
To < 4 kV	Medium (e.g., desktop computer)	36†	36	N/A‡	38
To < 4 kV	Small (e.g., telephone)	36§	36	38§	38
None	Larger (e.g., floor standing cabinet)	36 37	36 37	38 39	38 39
None	Medium (e.g., desktop unit)	36† 37†	36 37	N/A‡	38 39
None	Small (e.g., telephone)	36† 37†	36 37	38§ 39§	38 39

*Numbers in the table refer to figure numbers in the text of the guide.
†Slightly reduced amplitudes and durations.
‡Desktop or benchtop equipment is unlikely to be the victim of a direct furniture discharge, but it is as likely as any other equipment to be the victim of an indirect furniture discharge.
§Significantly reduced amplitudes and durations. Small receptors can be the victims of direct furniture discharge when they are hand-held.

9. Bibliography

This bibliography specifically relates to the charging and discharging process, *not* to ESD testing of equipment, which merits its own larger listing and which is not included in the scope of this guide.

[B1] ANSI PC63.16/D10, Draft Guide for Electrostatic Discharge Test Methodologies and Criteria for Electronic Equipment.[9]

[B2] Berbeco, G. R., "Static Protection 1. Causes of Static Charge Development and Effects on Electronic Devices," *Insulation/Circuits*, vol. 2b, no. 3, pp. 20–22, Mar. 1980.

[B3] Berta, I. and Gasteneh, N., "The Energy of Electrostatic Discharges," *Electrostatics,* pp. 67–72, 1979.

[B4] Blinde, D. and Lavoie, L., "Quantitative Effects of Relative and Absolute Humidity on ESD Generation," in *Proceedings of the EOS/ESD Symposium EOS-3*, pp. 9–13, 1981.

[B5] Bush, D. R., "Statistical Considerations of Electrostatic Discharge Evaluations," in *Proceedings of the 7th International EMC Symposium*, pp. 487–490, 1987.

[B6] Calderbaur, J. M., Overbay, D. E., and Snyder, H. Z., "The Effects of High Humidity Environments on Electrostatic Generation," in *Proceedings of the EOS/ESD Symposium EOS-2*, pp. 12–16, 1980.

[B7] Calvin, H., Hyatt, H., Mellberg, H., and Pellinen, D., "Measurement of Fast Transients and Application to Human ESD," in *Proceedings of the EOS/ESD Symposium EOS-2*, pp. 225–230, 1980.

[B8] Dhondy, N. and Reed, E. W., "Uniform Detection of Electrostatic Discharge Energy Using a Transient Plate (Computer Frame Protection)," *IBM Technical Disclosure Bulletin*, vol. 23, no. 4, pp. 1535–1536, 1980.

[B9] DiPlacido, J., Shih, C. H., and Ware, Brenden J., "Analysis of the Proximity Effects in Electric Field Measurement," *IEEE Transactions on Power Apparatus and Systems*, vol. PAS-97, no. 6, pp. 2167–2177, Nov.-Dec. 1978.

[B10] Durgin, D. L., Pelzl, R. M., Thompson, W. H., and Walker, R., "Survey of EOS/ESD Data Sources," in *Proceedings of the EOS/ESD Symposium EOS-4*, pp. 49–55, 1982.

[B11] Freund, T., "Tribo-Electricity," *Advanced Colloid and Interference Science* (Netherlands), vol. 11, no. 1, pp. 43–66, Feb. 1979.

[B12] Gallo, C. F. and Ahuja, S. K., "Electrification by Contact Charge Exchange: A Literature Survey of Microscopic Models," *IEEE Transactions on Industry Applications*, vol. IA-13, no. 4, pp. 348–345, Jul.-Aug. 1977.

[B13] Gerbi, G., Mensa, M., and Golzio, D., "Characterization of Electrostatic Discharge Transients," RCE-2163, ESA-CR (P)-1523, NASA, Washington, DC, p. 144, Oct. 1980.

[B14] Greason, W., *Electrostatic Damage in Electronics Devices and Systems*. Letchworth, Hertfordshire, England: Research Studies Press Ltd., 1987.

[9]This authorized standards project was not approved at the time this guide went to press.

[B15] Greason, W., "Effect of Discharge Electrode and Body Geometry on the Relative Probability and Severity of the ESD Event in Electronic Systems," in *Proceedings of the IEEE IAS Annual Meeting*, 1988.

[B16] Greason, W., "Review of the Effect of Electrostatic Discharge and Protection Techniques for Electronic Systems," *IEEE Transactions on Industry Applications*, vol. IA-23, no. 2, pp. 205–216, 1987.

[B17] Honda, M., "A New Threat EMI Effect by Indirect ESD on Electronic Equipment," in *Proceedings of the IEEE/IAS Conference*, pp. 1647–1679, 1987.

[B18] Honda, M. and Takeyoshi, K., "ESD Characteristics and Their Effects on Computers," *Electromagnetic Communications Journal*, vol. 83, no. 209, pp. 25–30, Dec. 1983; vol. 83, no. 292, pp. 13–17, Mar. 1984; vol. 85, no. 86, pp. 39–42, Jul. 1985; vol. 86, no. 107, pp. 17–22, Jul. 1986.

[B19] Jones, L. A. and Makin, B., "Measurement of Charge Transfer in a Capacitive Discharge," *IEEE Transactions on Industry Applications*, vol. IA-16, no. 1, pp. 76–79, Jan.-Feb. 1980.

[B20] Kawamara, T., "Acceleration of Spark Formation in the Discharge of an ESD Simulator by Using a Charge Injection Capacitor," in *Proceedings of the 7th International EMC Symposium*, pp. 481–486, 1987.

[B21] Kohlhass, P., "Controlling Potential Static Charge Problems," *Electronic Production* (GB), vol. 6, no. 5, pp. 15–17, 19, 21, 1977.

[B22] Kunz, H. A., "Electrostatic Charging and Simulation of the Discharging Process," in *Proceedings of the IEEE International Symposium on EMC*, pp. 206–210, 1982.

[B23] Liu, B. Y., Pui, D. Y., Kinstley, W. D., and Fisher, W. G., "Aerosol Charging and Neutralization and Electrostatic Discharge in Clean Room," *Journal of Environmental Sciences*, vol. 30, no. 2, pp. 42–46, Mar.-Apr. 1987.

[B24] Mahmoud, I.S., "Electrostatic Discharge Shielding," *IBM Technical Disclosure Bulletin*, vol. 23, no. 7B, p. 3076, Dec. 1980.

[B25] Marble, A. E., MacDonald, A.C., McVicar, D., and Roberts, A., "A Measurement of the Electrostatic Voltage, Capacitance and Energy Storage Characteristics of the Human Body (Explosion Hazard)," *Physics, Medicine, Biology*, vol. 22, no. 2, pp. 365–367, Mar. 1977.

[B26] Mardiguian, M., "Recent Developments in the Understanding of Coupling Paths of ESD through a Metallic Cabinet," in *Proceedings of the 6th EMC Symposium*, pp. 31–34, 1985.

[B27] Mardiguian, M., "ESD Testing, The need for a dual personal and material discharge simulation," in *Proceedings of the 7th EMC Symposium*, pp. 473–476, 1987.

[B28] Molyneux Child, J.W. and DeVoil, G.F., "Human Equivalent Circuit for Static Discharge," *Electronic Industries (GB)*, vol. 7, no. 5, p. 37, May 1981.

[B29] Rhoades, W. T., "Achieving ESD Equipment Protection with Emission Control," in *Proceedings of the IEEE International Symposium on EMC*, pp. 232–237, 1985.

[B30] Sperber, W. and Blink, R.P., "Characterization of Electrostatic Discharge Generated by an Occupant of an Automobile," in *Proceedings of the IEEE International Symposium on EMC*, pp. 360–370, 1987.

[B31] Sullivan, S. S. and Underwood, D.D., "Automobile Environment: Its Effects on the Human Body ESD Model," in *Proceedings of the EOS/ESD Symposium EOS-7*, pp. 103–106, 1985.

[B32] Werner, Gosta, "Studies of the Electrostatic Fields and the Onset Voltages of Different Types of High Voltage Conductors and Screen Electrodes by the Method of Simulated Charges," Dissertation, Chalmers University of Technology, Goetborg, Sweden.

[B33] Wild, N. and Coakley, P., "Evidence for Discrete Plasma Emission During Dielectric Discharge Events," *IEEE Transactions on Nuclear Science*, vol. NS-31, no. 6, pp. 1591–1593, Dec. 1984.

[B34] Wu, C., McCarthy, W. F., Chong, Y., and Rudko, M., "On the Limitations of ESD Simulators," in *Proceedings of the IEEE International Symposium on EMC*, pp. 371–373, 1987.

[B35] Wu, C., McCarthy, W. F., Chang, Y., and Rudko, M., "On the Penetration of ESD Current," in *Proceedings of the IEEE International Symposium on EMC*, pp. 374–378, 1987.

Appendixes

(These appendixes are not a part of IEEE Std C62.47-1992, IEEE Guide on Electrostatic Discharge (ESD): Characterization of the ESD Environment, but are included for information only.)

Appendix A
Static Decay, Surface and Volume Resistivity, and Triboelectric Series

Static decay measurements are often made by charging the material of interest alternately to +5000 VDC and -5000 VDC, and measuring the decay time to 0 V in a controlled environment. Because of the difficulties associated with measurements of "zero volts," investigators frequently use cutoff points such as 10% of the original charge voltage.

Surface resitivity is measured in ohms per square, and volume, or bulk, resitivity is measured in ohm-centimeters.Documents often specify the use of a 500 VDC test voltage and an electrification time of 60 s before recording the resistance value. The test methods define various fixture configurations along with the associated calculations required for true readings. A major source of error is due to fringing effects at the edges of measurement fixture electrodes. The use of a concentric circular fixture or other improved versions overcomes the "fringing effect" problem.

For the purpose of ESD protective materials qualification, surface resistivity or volume resistivity measurements should be performed at the lowest relative humidity anticipated in the usage environment. Hygroscopic material will show significant variations in surface resitivity with relative humidity, particularly at low values of relative humidity.

A number of common materials are contained in the triboelectric series of Table A1. Materials higher up in the series will generally develop a positive charge relative to materials listed lower in the series. The farther apart the materials are in the series, the greater will be the magnitude of the static charge developed.

The order of ranking in a triboelectric series is not fixed. It is not always possible to duplicate a series in the same order. Further, the separation on a triboelectric series chart does not necessarily indicate the magnitude of the charge assumed by a substance due to triboelectric charging. The order and degree of charge depends on many factors such as surface cleanliness, ambient conditions, pressure of contact, speed of rubbing or separation, and the surface area over which the rubbing occurs.

Table A1
Triboelectric Series [9]

Materials	Polarity
Asbestos	Positive
Acetate	Positive
Glass	Positive
Human hair	Positive
Nylon	Positive
Wool	Positive
Fur	Positive
Lead	Positive
Silk	Positive
Aluminum	Positive
Paper	Positive
Polyurethane	Positive
Cotton	Positive
Wood	Positive
Steel	Positive
Sealing wax	Positive
Hard rubber	Positive
Mylar	Positive
Epoxy glass	Positive
Nickel, copper, silver	Positive
Brass, stainless steel	Positive
Synthetic rubber	Positive
Acrylic	Positive
Polystyrene foam	Positive
Polyurethane foam	Positive
Polyester	Positive
Saran	Positive
Polyethylene	Positive
Polypropylene	Positive
PVC (Vinyl)	Negative
Teflon	Negative
Silicon rubber	Negative

Appendix B
Additional Background on Specific ESD Phenomena

B1. Fast-Rise Initial Current Pulse; Effects on Electronic Equipment

B1.1 Fast-Rise Initial Current Pulse. It has been supposed, but not as yet proven, that the difference between discharges with and without the initial current pulse or a steep initial slope may relate to absence or presence of significant corona, or partial discharge, at the time of the ESD. The correlation between the existence of the initial pulse in a human ESD and the absence of significant corona has been assumed because of the apparent correspondence between conditions conducive to the existence of the pulse with those conducive to the absence of significant corona. Among the most important of these conditions is the presence of rounded (as opposed to sharp) electrodes, particularly in conjunction with charge voltage in the low kilovolt range. Measurements made with sharp electrodes show both earlier inception of corona versus increasing charge voltage and earlier disappearance of the initial spike with increasing charge voltage [26]. However, while the existence of the initial pulse and the absence of significant corona seem to track in this general way, a cause-and-effect relationship between the two phenomena has not been proven.

A related explanation for the gradual disappearance of the initial current spike with increasing charge voltage depends on the relationship of the voltage between the intruder and the receptor at the time of the ESD, as a function of the spacing between their respective electrodes at the same point in time. For any given distance between two electrodes of specific shapes, in a particular gas or combination of gases such as air, there is a minimum voltage required to establish a discharge arc. This minimum voltage is the static breakdown voltage for the electrode spacing. The maximum spacing at which a discharge will occur for a given voltage is the critical spacing, or critical distance, for that static breakdown voltage. (Both the static breakdown voltage and the critical distance depend on many factors, including electrode shapes, composition of the gas, temperature, humidity, and so on.)

If, due to a fast approach speed, the discharge does not take place until the actual voltage significantly exceeds the static breakdown voltage, then when the discharge actually does take place, the avalanche process is accelerated and the rise time of the discharge current wave will be much faster than if the discharge takes place just at the static breakdown voltage. Obtaining a steep initial slope may thus require what might be termed an overvolted gap [16]. The possible correlation between this mechanism and corona dependence is that the existence of significant corona will prevent overvoltage of the gap.

B1.2 Rise Time Versus Effects on Electronic Equipment. The importance of the fast rise time of the ESD current wave in regard to equipment ESD immunity has been investigated in some detail.

The authors of [15] performed tests to determine upset levels for a number of electronic equipments of what they termed "medium" susceptibility to ESD. Their tests included ESD from actual hand/metal ESD events and from five ESD testers of different designs. The relatively high sensitivity of this equipment to steep initial slope may be inferred from comparison of the hand/metal test results with results of tests using the five ESD testers. These five testers included four commercially available air discharge ESD simulators and a relay-operated, so-called contact mode simulator designed by the authors of [15]. All four of the commercially available simulators were designed as air discharge simulators to the same ESD test standard (the 1984 version of [1]).

Distribution of initial slope versus charge voltage for the hand/metal tests is shown in Fig B1. The data in that figure were taken for a planned distribution of approach speeds at each charge voltage: 10% of the tests were performed using approach speeds that were as fast as

possible, 10% with approach speeds that were extremely slow, and 80% were executed using approach speeds designed to simulate what might be termed an "average" human approach speed. Fig B1 shows means, standard deviations, and observed extreme values of initial slope in amperes/nanoseconds of the leading edge of the current wave for a series of hand/metal ESDs. (Initial slope is referred to as rising slope in [15].) There is a wide range of initial slopes for each charge voltage. In Fig B1, it varies from 5–32 A/ns at a charge voltage of 4 kV, from 7–61 A/ns at 8 kV, and from 15–90 A/ns at 16 kV. This means the normalized rising slope at 4 kV is actually larger than at 16 kV (i.e., at 4 kV the normalized rising slope is about 5.75 A/μs/kV, and at 16 kV the normalized rising slope is about 3.8 A/ns/kV). (This would seem to indicate that the conditions of this study resulted in relatively slow rising slopes at lower voltages and faster-than-normal rising slopes for high voltages.)

Distributions of initial slope versus charge voltage are shown in Figs B2 through B5 for the four commercially available air discharge simulators, identified in the figures as simulators A, B, C, and D, respectively. None of the testers displayed initial slope distributions that were consistently as steep over the full voltage range as those of the hand/metal ESDs of Fig B1. The distribution of initial slope versus charge voltage is shown in Fig B6 for the relay- operated simulator designed by the authors of reference [15]. Its initial current slopes are comparable with those of the hand/metal ESD events of Fig B1.

Failure distributions are presented in Figs B7, B8, and B9 for three different items of equipment under test (EUT) respectively, using actual hand/metal (Fig B1), the four air discharge simulators (Figs B2 through B5) and the contact-simulator (Fig B6). (The authors omitted data for simulator B from Fig B7, and for simulators C and D from Fig B8. They provided no information on the omissions.)

For EUT #1, whose failure distribution is shown in Fig B7, slow simulators A, C, and D gave good, fair, and poor replications, respectively, of the hand/metal failure distribution versus charge voltage. Also from Fig B7, the fast, relay-operated simulator gave higher failure rates than those obtained with real hand/metal ESD events. For EUT #2, whose failure distributions are shown in Fig B8, however, both slower simulators A and B gave far lower failures than did actual hand/metal ESD events. Again in Fig B8 for EUT #2, the fast simulator gave a better approximation to the failure distribution of actual hand/metal ESD events, although again showing somewhat more failures than hand/metal. Finally, the failure distributions for EUT #3 are shown in of Fig B9. This equipment showed no failures whatsoever with slow simulators A, B, and D. It showed some failures with slow simulator C at lower voltages, but few failures at higher voltages.

Finally, Fig B9 for EUT #3 shows that the fast ESD simulator gave a failure distribution reasonably close to the high failure rate distribution of hand/metal ESD events.

The authors of [15] concluded that for the three equipments chosen for the tests, initial slope could be a key factor in producing failures due to ESD.

It should be noted parenthetically that the degree to which an ESD simulator replicates the effects of actual hand/metal ESD events depends on the nature of the EUT and varies with simulator design. ESD simulation is a statistical process; accordingly, the data presented by Figs B1 through B9 are representative of real experience.

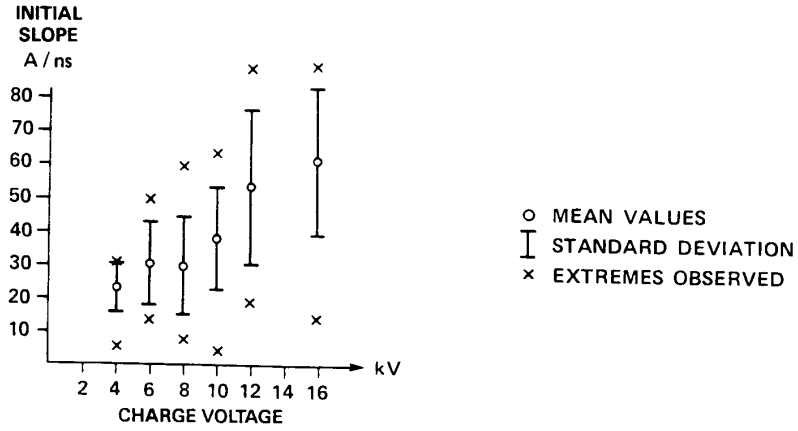

Fig B1
Initial Slope Versus Charge Voltage for Hand/Metal ESD [15]

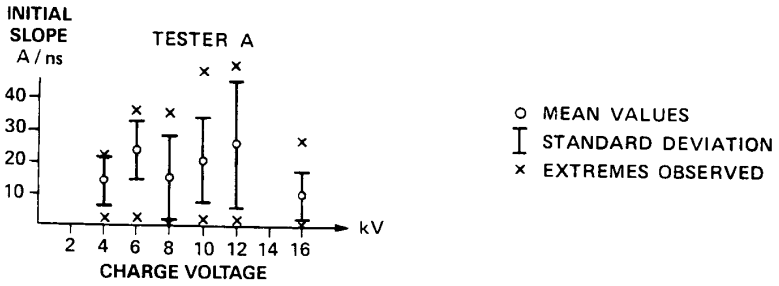

Fig B2
Initial Slope Versus Charge Voltage for ESD Tester A [15]

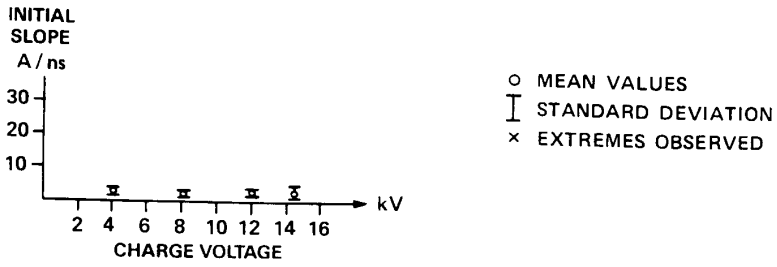

Fig B3
Slope Versus Charge Voltage for ESD Tester B [15]

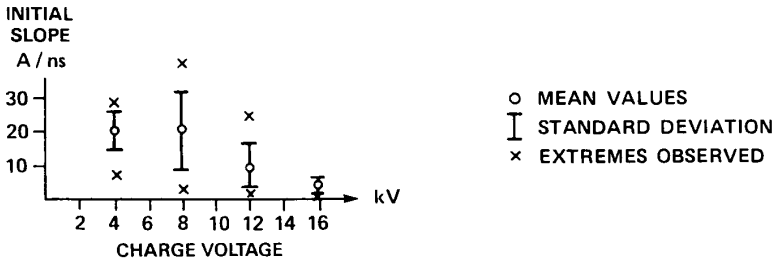

Fig B4
Rising Slope Versus Charge Voltage for ESD Tester C [15]

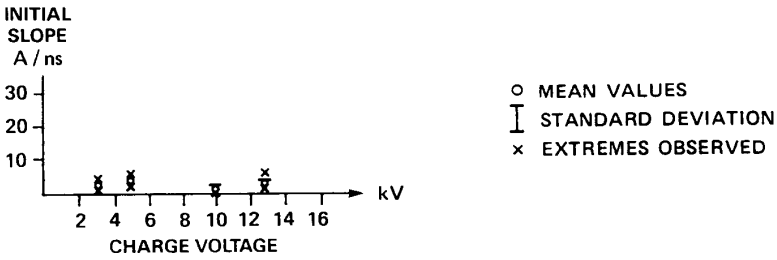

Fig B5
Slope Versus Charge Voltage for ESD Tester D [15]

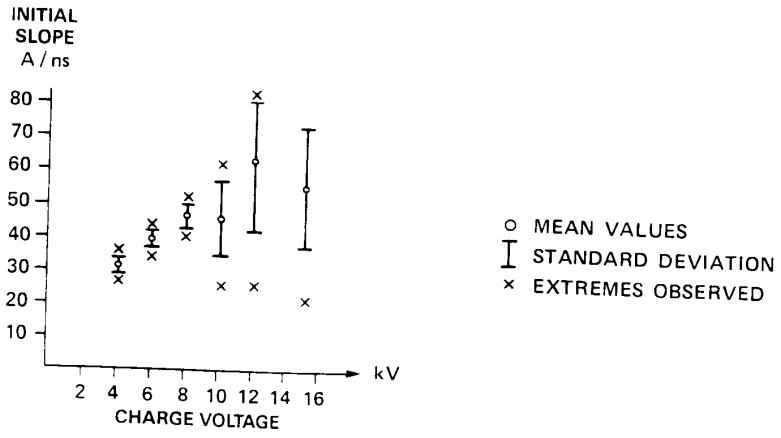

Fig B6
Initial Slope Versus Charge Voltage for Fast-Rise Time, Relay-Operated ESD Tester E [15]

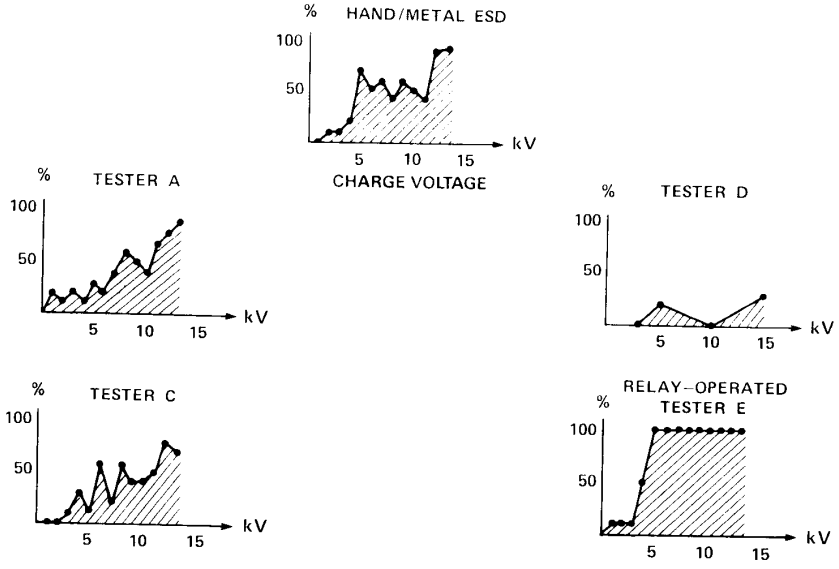

Fig B7
Failure Probabilities With EUT #1 [15]

NOTES: (1) Percent failures versus charge voltage.
(2) The authors of [15] omitted tester B from this figure.

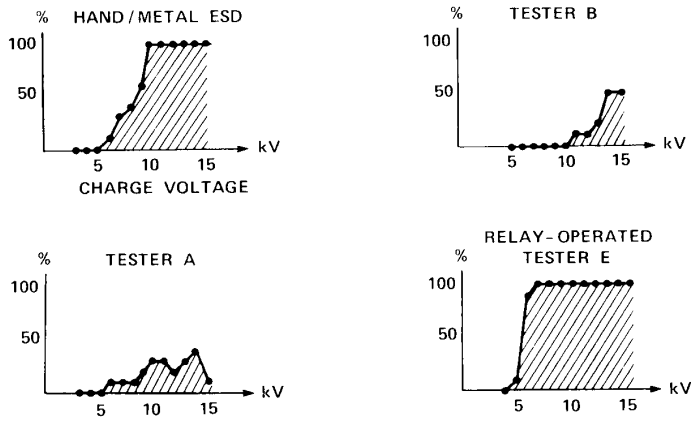

Fig B8
Failure Probabilities With EUT #2 [15]

NOTES: (1) Percent failures versus charge voltage
(2) The authors of [15] omitted testers C and D from this figure.

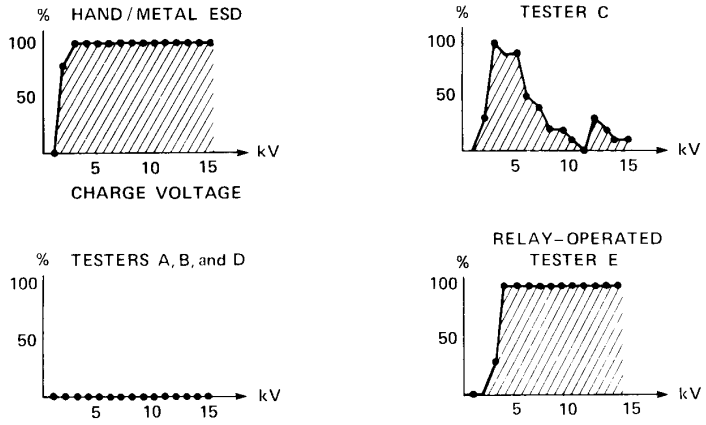

Fig B9
Failure Probabilities With EUT #3 [15]

NOTE: Percent failures versus charge voltage.

B2. Initial Slope Versus Approach Speed and Other Variables

A definitive series of tests have been performed to relate initial slope to approach speed and charge voltage [13]. Experiments using motor-driven electrodes permitted controlled and repeatable approach speeds, which were used to determine the sensitivity of initial slope to approach speed for a given charge voltage. Results of these tests for 4 kV, 8 kV, and 16 kV are

shown in Figs B10, B11, and B12, respectively. There are essentially three zones of approach speed at any charge voltage, as follows:

Zone A: From the smallest speed possible to a first threshold, the initial slope is below 10 A/ns and the dispersion of initial slopes is relatively small.

Zone B: Initial slopes increase and the dispersion of initial slopes is very high.

Zone C: The initial slope is limited due to the rise-time limitation of the measurement system (400 MHz in [13]). Dispersion of the initial slopes in this zone is markedly lower than in Zone B, but rise time limitations make it difficult to infer actual slope figures in this zone. It is therefore assumed that at least some initial slopes are greater than those that were measured.

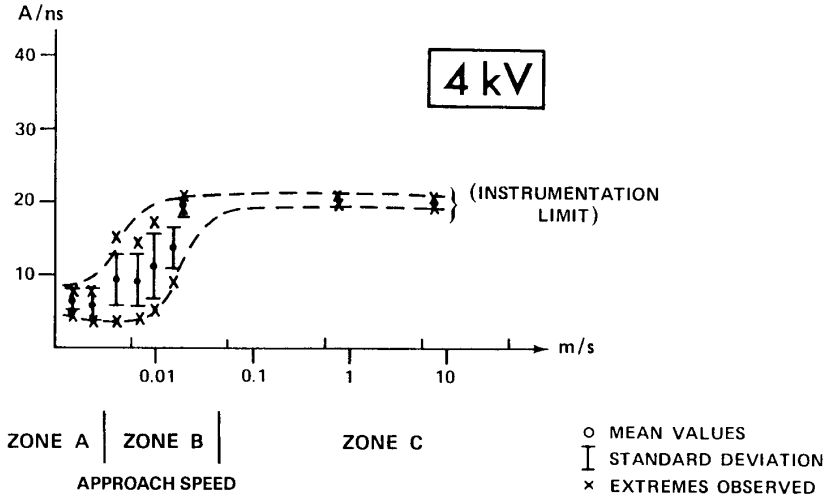

Fig B10
Initial or Rising Slope Versus Speed of Approach for 4 kV Charge Voltage [13]

It is extremely important to note that the horizontal line in Figs B10 and B11 termed "instrumentation limit" is drawn to avoid confusion, above the highest indicated measurement points.

In point of fact, the authors of [13] later indicated that the initial slope limitation in some or all of those highest indicated measurement points was caused by the instrumentation limit. The line could better have been left undrawn, or else drawn on a level with the highest measurements. Also note that even those points that lie just below the limit may have been affected by it, i.e., their measured slopes may have been reduced by the instrumentation limit even though they had not quite reached it. This is particularly important also in connection with Fig B12, in which no instrumentation limit line was specifically included by the authors, but in which the measured initial slopes are obviously slowing down as they approach the instrumentation limit that is only implicit in this particular figure due to the parameters

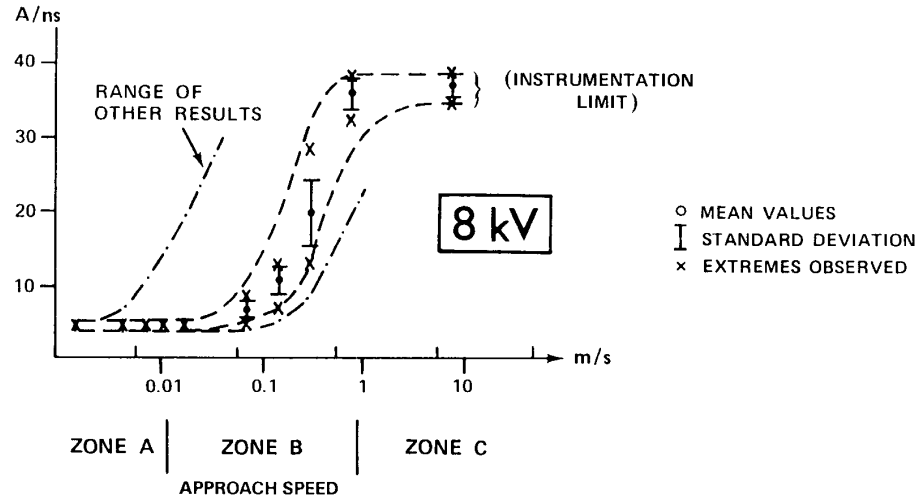

Fig B11
Initial or Rising Slope Versus Speed of Approach for 8 kV Charge Voltage [13]

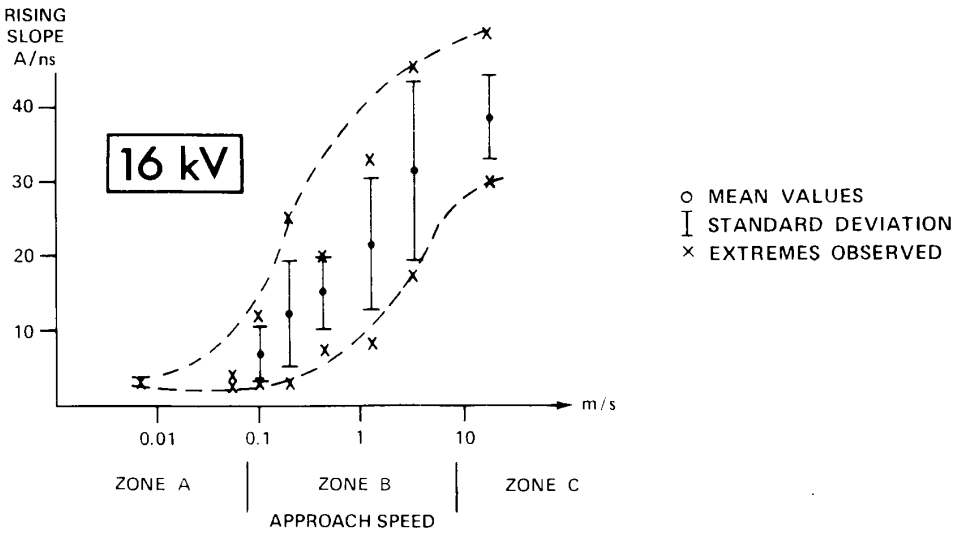

Fig B12
Speed of Approach—
Initial or Rising Slope Versus Speed of Approach for 16 kV Voltage [13]

involved. Also, it should be noted that the instrumentation limit in this series of tests was evidently not the same as for the investigation of B1.2.

Therefore, precise information about the rising slope is not totally consistent for B1.2 and B2. However, the basic concepts and trends described are not in conflict.

The authors of [13] note that "The statistical result and the limits of Zone B are not stable. They depend on various external conditions. The result of the 8 kV tests of Fig B11, for example, which shows a relatively small dispersion in Zone B, is the result of a measurement series made immediately after cleaning and polishing the two parts forming the spark gap. As the surface gets worn out, the spread of the results increases (second line in Fig B11). The result also depends on humidity and other conditions. Breathing into the spark zone, for example, shifts the result significantly."

The authors of [13] continue, "The speed of approach, either when a person touches an EUT with a metallic object or using the test generator, is normally in the range of 0.01–0.5 m/s. For voltages between 4 kV and 16 kV, this speed is just in the transition Zone B where the results are very unstable. Keeping the speed of approach constant (therefore) does not lead to constant rising slopes." Variations in the speed of approach and other variables can lead to a variation of the rising slope by a factor of 20 or more.

B3. Multiple Discharges

As indicated in 6.4.4, the pulses in a multiple ESD event are spaced by tens of microseconds up to tens of milliseconds.

It is considered doubtful that this wide disparity in time delays would occur if all multiple discharges had the same cause; at least two explanations are probably necessary, one for each range of time interval.

An attempt has been made to explain the shorter intervals by postulating that the capacitance of the arm and body is partially recharged, after a discharge, from the charge stored in a layer between the feet and shoe dielectric [10].

A 100 kΩ to 200 kΩ skin impedance connecting the charge layers and the body could account for a recharge time constant in the range of several microseconds, and the ratio of capacitance for the two sections would determine the relative level of the charge voltage for each successive discharge in a series. The impedance of most body tissues is not very high, but skin resistance can be as high as 1 MΩ; so an impedance of hundreds of kilohms is theoretically possible. The capacitance in this layer can also be quite large because of the close proximity of the skin to the shoe dielectric.

The longer intervals have been explained by two possible mechanisms. The first is dielectric hysteresis of the intruder capacitance, perhaps of the shoe leather (or other material) that acts as a dielectric for a major portion of the human body capacitance [10]. The second possible mechanism, and the one that is the most probable cause of widely spaced multiple discharges, is the phenomenon that, when the intruder approaches the receptor, the discharge from the intruder is extinguished when current drops below a few tenths of an ampere (roughly the range of arc extinction in air). A continuing approach will reignite the arc at the critical distance for the remaining voltage, and so on. Physical approach speeds of several meters per second can provide a rationale for intervals of milliseconds to tens of milliseconds resulting from successive arc extinction and reignition.

Multiple ESDs are analogous to multiple strokes in a single lightning flash, a well-recognized phenomenon in the field of lightning research. As multiples become more widely recognized in conjunction with ESD, it may be useful to adopt nomenclature analogous to that used for lightning: an ESD flash would describe the set of multiple discharges occurring in a single approach of an intruder towards a receptor, with each individual discharge described as an ESD stroke. Use of the terms ESD event flash and ESD event stroke are natural extensions of this suggested nomenclature.